Effects of neutrino heating and g-mode on SASI with steady-state initial conditions

Naofumi OHNISHI

Center for Research Strategy and Support, Tohoku University
Department of Aerospace Engineering, Tohoku University

Phone&Fax: +81-22-795-6919
E-mail: ohnishi@rhd.mech.tohoku.ac.jp

Asymmetry Instabilities in Stellar Core Collapse
June 30-July 11, 2008
Institut Henri Poincaré, Paris, France

Radiation hydrodynamic simulations have been conducted for applications of laser produced plasmas and other hypersonic flows

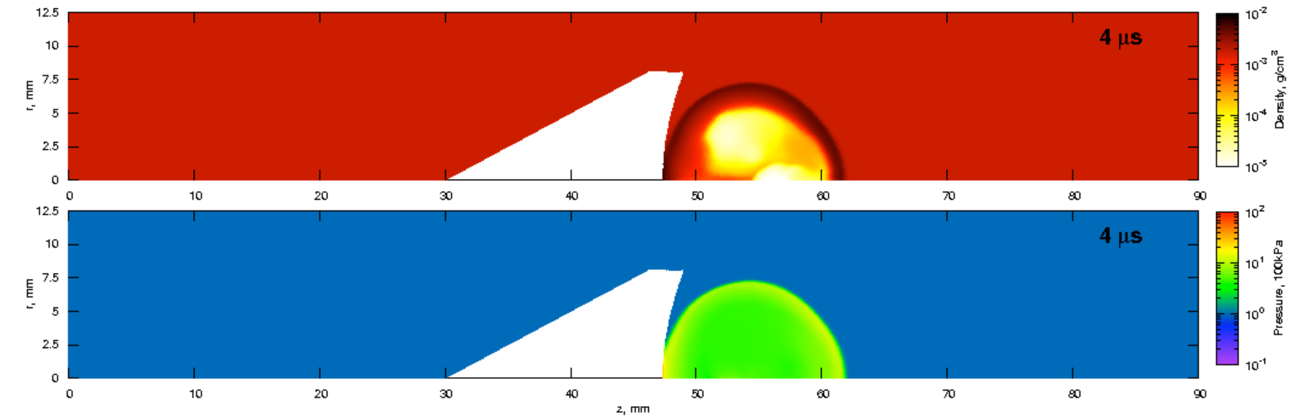

Ohnishi et al. (2006)

- **Laser propulsion**
- **Hydrodynamic instabilities in ICF target**
- **High-temperature plasma as x-ray source**
  - **low-density aerogel**
  - **plasma medium for x-ray laser**

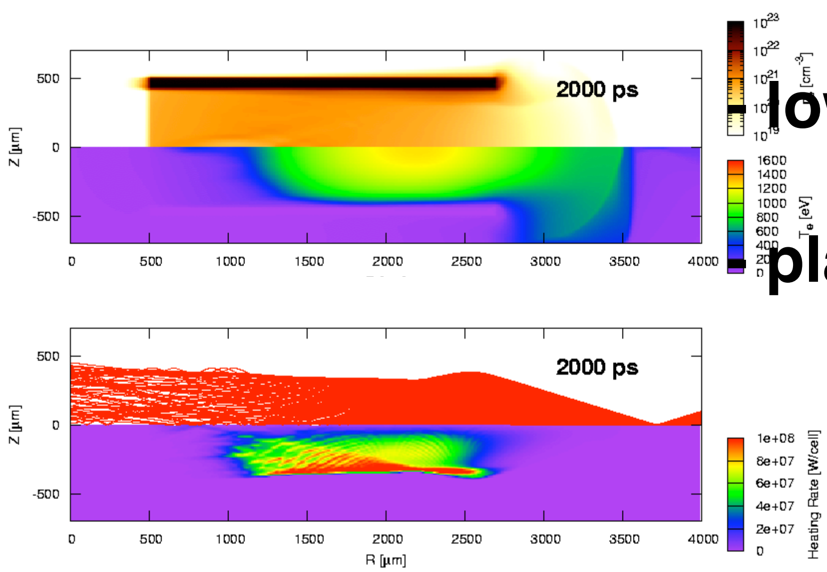

Tanabe et al. (2007)

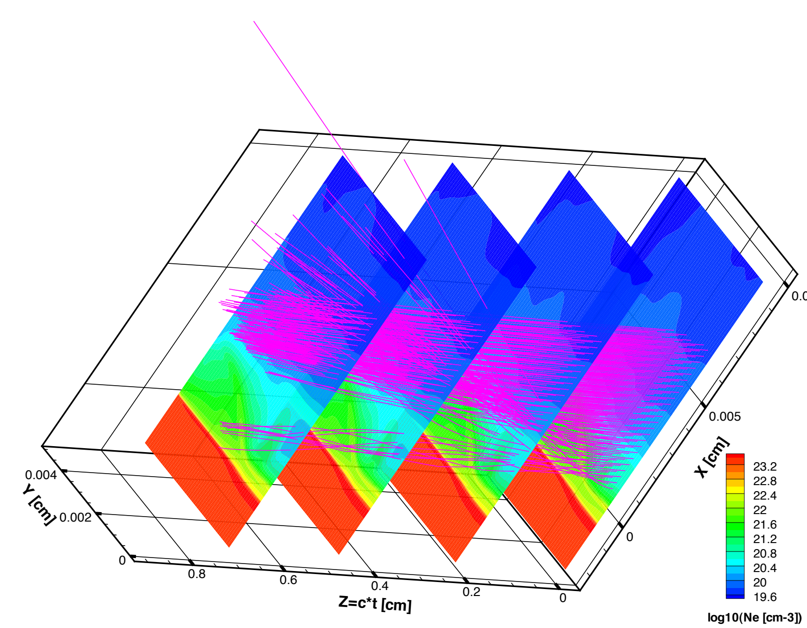

Ohnishi et al. (2005)

SUMMARY

Standing accretion shock instability has been investigated by 2D axisymmetric simulations with steady-state solution

- **Linear growth of the perturbation was found for low-l modes with neutrino heating**
- **2D axisymmetric simulations suggest that SASI can trigger the explosion from the stalled shock wave**
- **Additional neutrino heating of neutrino-He inelastic scattering is enhanced by SASI but may play a minor role on a successful explosion**
- **It seems to be difficult that the pressure perturbation which is mimic of g-mode excites SASI due to the impedance mismatch**

1D simulations can NOT succeed a core-collapse supernova explosion even with including neutrino heating

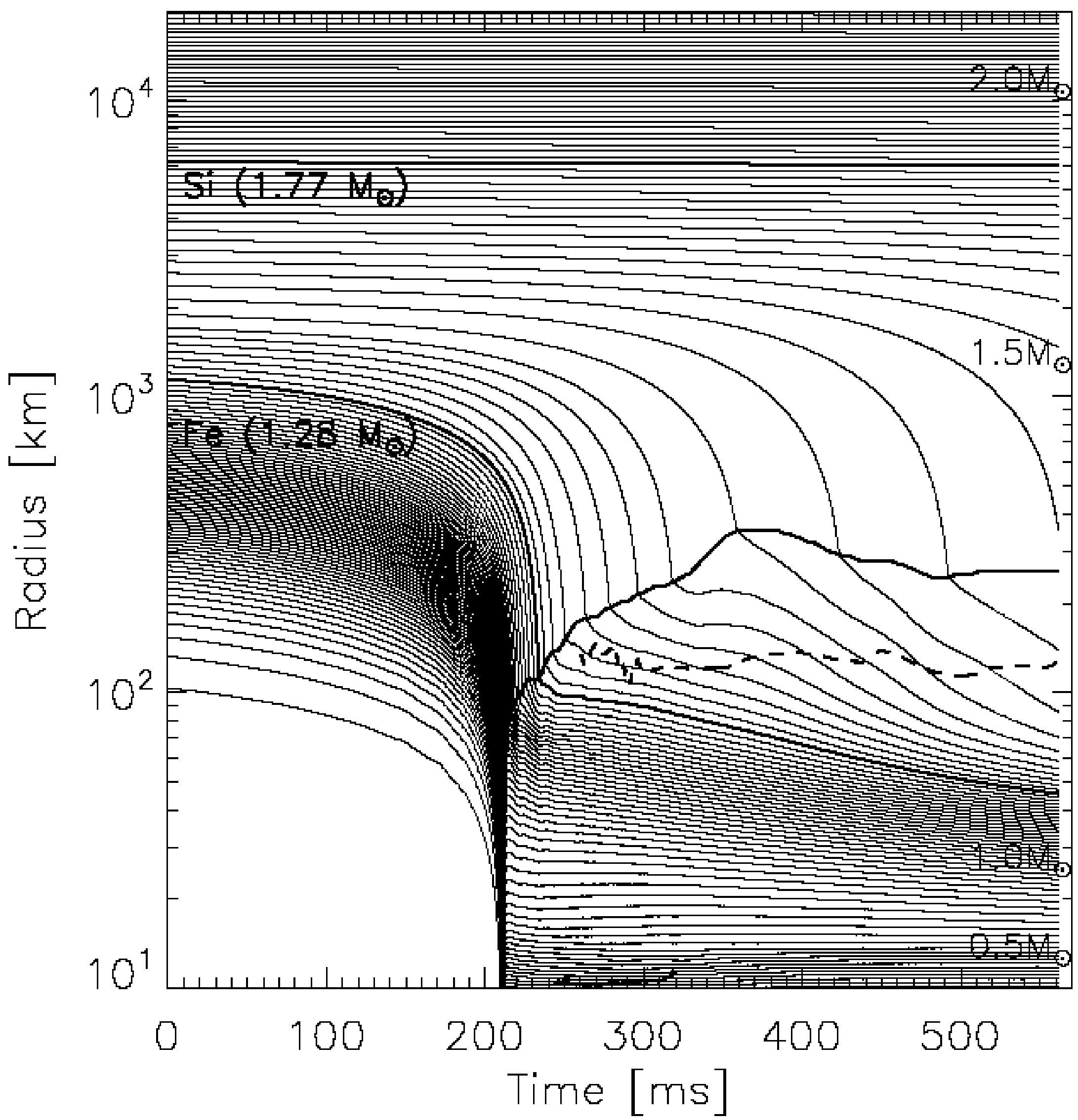

(Rampp et al. 2002)

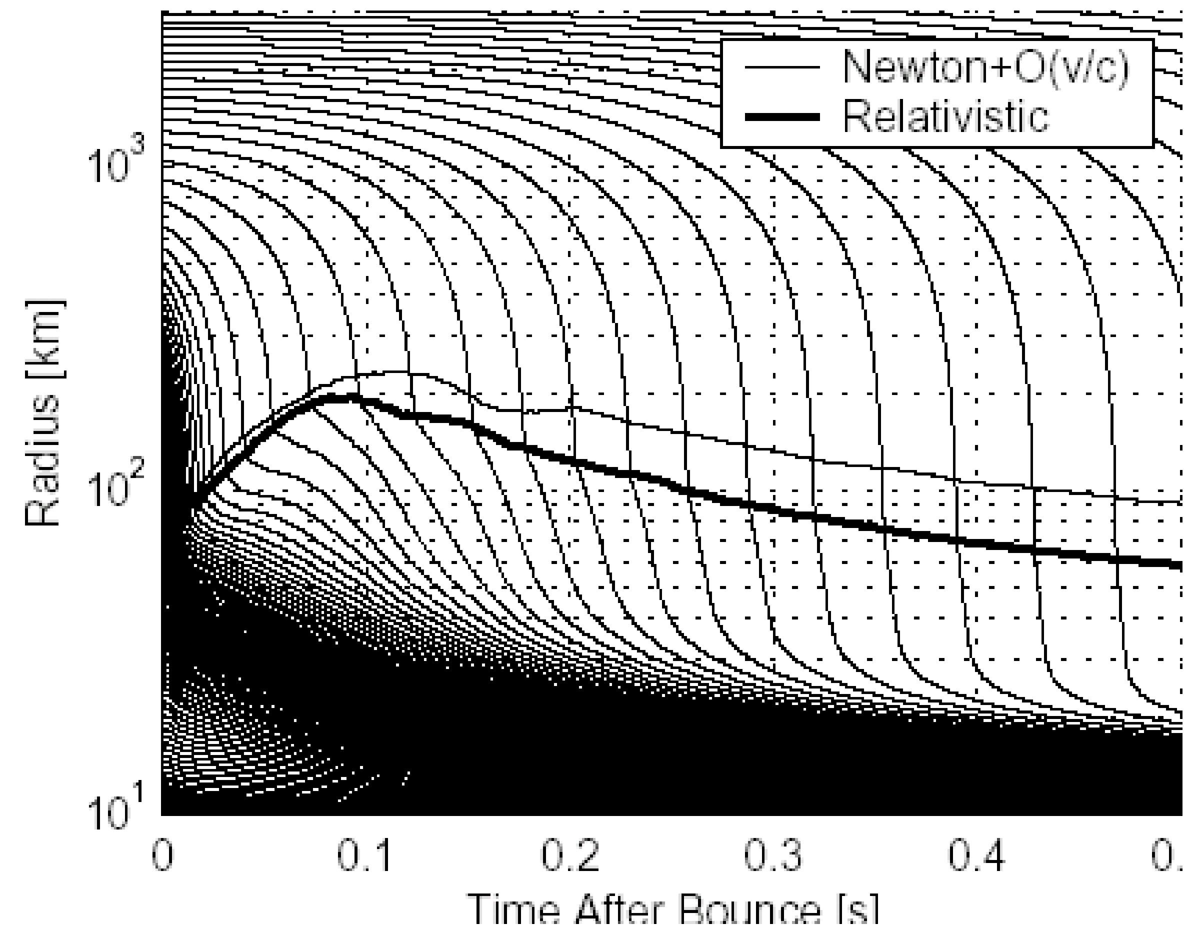

(Liebendörfer et al. 2002)

Any multi-dimensional effects are required to explain a core-collapse supernova explosion.

Standing Accretion Shock Instability (SASI) can be observed in adiabatic supernova simulations

- coupling between entropy wave and acoustic wave
- no neutrino heating (no convective instability)
- large evolution in low modes (l = 1, 2)

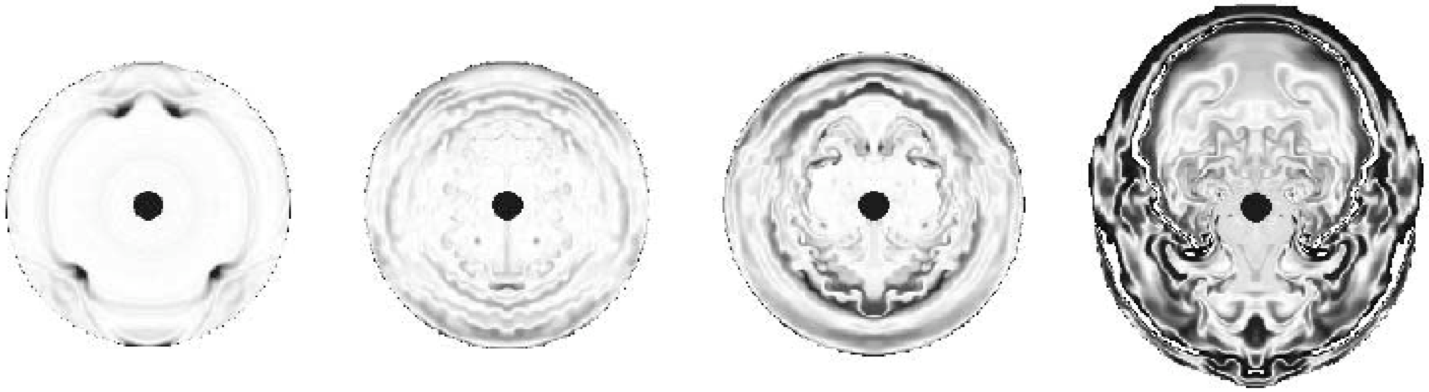

entropy contours

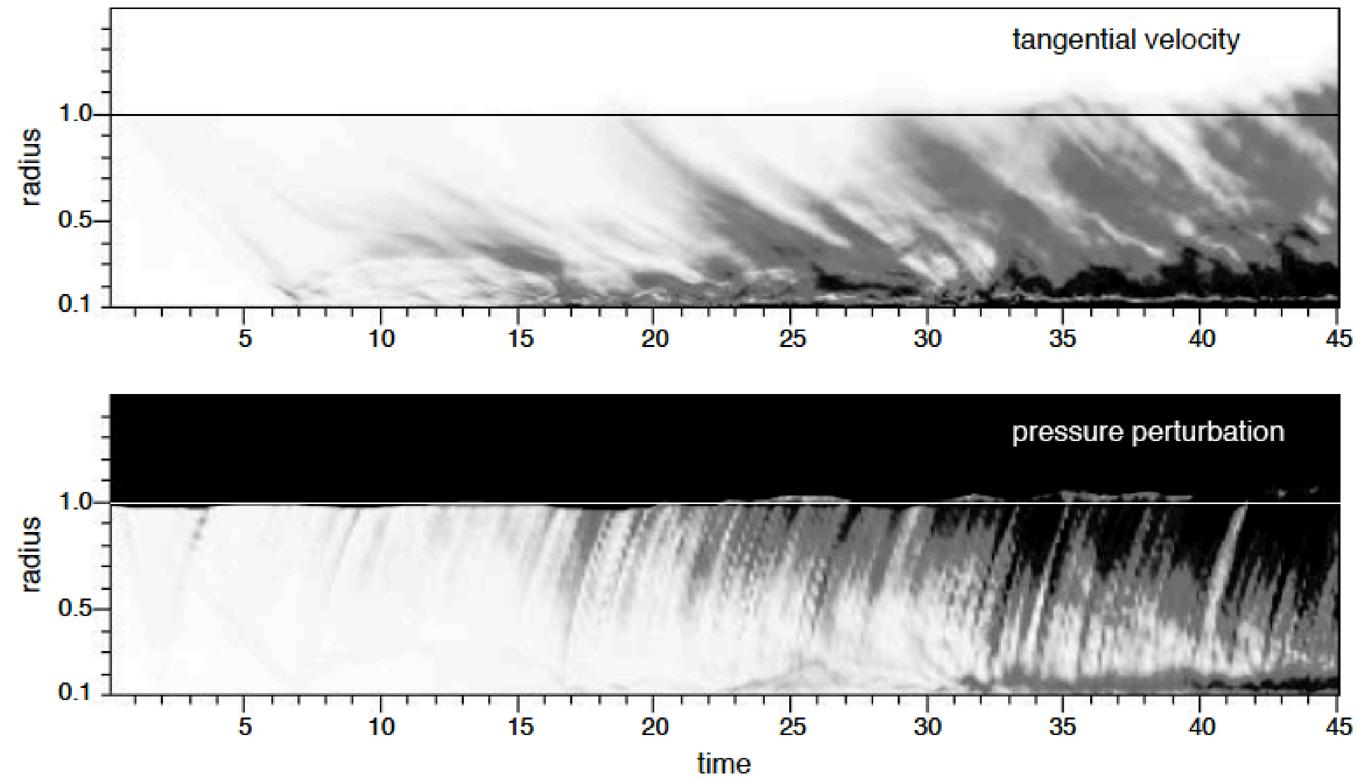

(Blondin et al. 2003)

Governing equations without self-gravity effect

- fluid equations and advection of electron fraction (electron mass conservation)

$$\frac{\partial \rho}{\partial t} + \nabla \cdot (\rho \boldsymbol{u}) = 0 \tag{1}$$

$$\frac{\partial (\rho \boldsymbol{u})}{\partial t} + \nabla \cdot (\rho \boldsymbol{u}\boldsymbol{u} + p) = -\rho \nabla \Phi \tag{2}$$

$$\frac{\partial (\rho \varepsilon)}{\partial t} + \nabla \cdot [(\rho \varepsilon + p)\boldsymbol{u}] = Q_{\mathrm{E}} + Q_{\mathrm{incoh}} \tag{3}$$

$$\frac{\partial Y_{\mathrm{e}}}{\partial t} + \boldsymbol{u} \cdot \nabla Y_{\mathrm{e}} = Q_{\mathrm{N}} \tag{4}$$

- gravitational potential due to neutron star mass M

$$\Phi = -\frac{GM}{r} \tag{5}$$

Heating of electron-type neutrino and antineutrino is taken into account assuming constant emission from central object

- heating rate and electron generation rate

$$Q_{\mathrm{E}} = -\frac{4\pi c}{(2\pi\hbar c)^3}\int_0^{\infty} \epsilon^3 \mathrm{d}\epsilon \left[j(\epsilon) - (j(\epsilon)+\kappa(\epsilon))\, f(\epsilon)\right]$$

$$Q_{\mathrm{N}} = i\frac{m_{\mathrm{B}}}{\rho}\frac{4\pi c}{(2\pi\hbar c)^3}\int_0^{\infty} \epsilon^2 \mathrm{d}\epsilon \left[j(\epsilon) - (j(\epsilon)+\kappa(\epsilon))\, f(\epsilon)\right]$$

$$\begin{cases} i = -1 & \text{(for electron-type neutrino)} \\ i = 1 & \text{(for electron-type antineutrino)} \end{cases}$$

- neutrino distribution function with given luminosity and temperature

$$L_\nu = \left(\frac{7}{16}\sigma T_\nu^4\right)\left(4\pi r_\nu^2\right)$$

$$f(\epsilon) = \left(\frac{1}{1+\exp(\epsilon/k_{\mathrm{B}}T_\nu)}\right)\frac{2\pi\left(1-\sqrt{1-(r_\nu/r)^2}\right)}{4\pi}$$

Initial profiles are determined by solving steady state equations (Yamasaki & Yamada 2005)

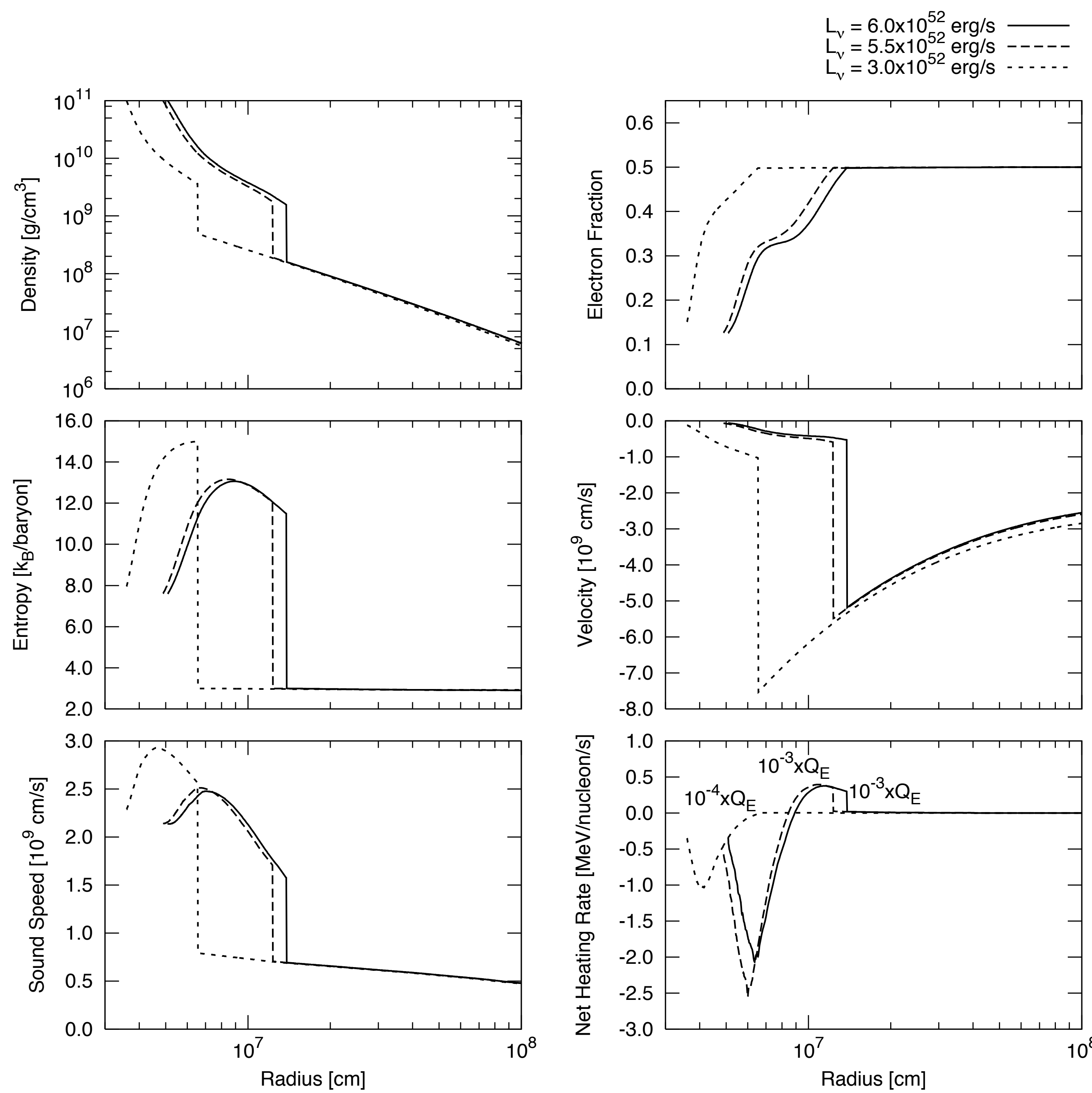

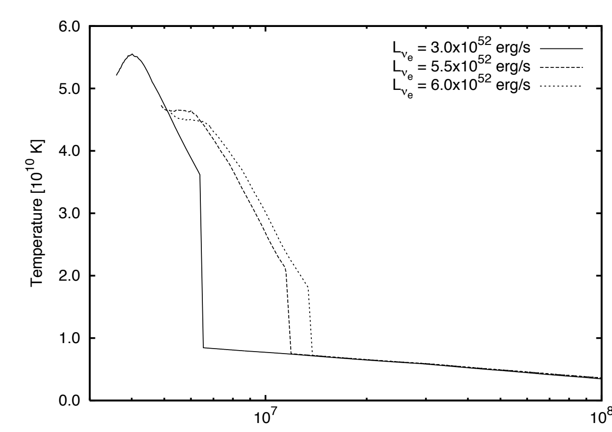

Numerical conditions

- axisymmetric (based on ZEUS-2D)
- tabulated EOS by Shen et al. (1998)
- fixed condition of the outer boundary with unperturbed state
- free outflow of the inner boundary except for the radial velocity

  $v_{r,0} = v_{r,1}(r_1^2/r_0^2)$ with constant $v_{r,1}$

  (other variables in the ghost mesh are copied with the most inner values)

- mass accretion rate and mass of the central object are fixed with

  $\dot{M} = 1\ M_\odot\ \mathrm{s}^{-1}$ and $M_{\mathrm{in}} = 1.4\ M_\odot$

- $T_{\nu_e} = 4$ MeV and $T_{\bar{\nu}_e} = 5$ MeV

- velocity perturbation is initially imposed on the whole flowfield

  $v_r(r,\theta) = v_r^{1\mathrm{D}}(r) + \delta v_r(r,\theta)$

SASI occurs also with neutrino heating and leads to explode with high neutrino luminosity

w/ 1% velocity perturbation

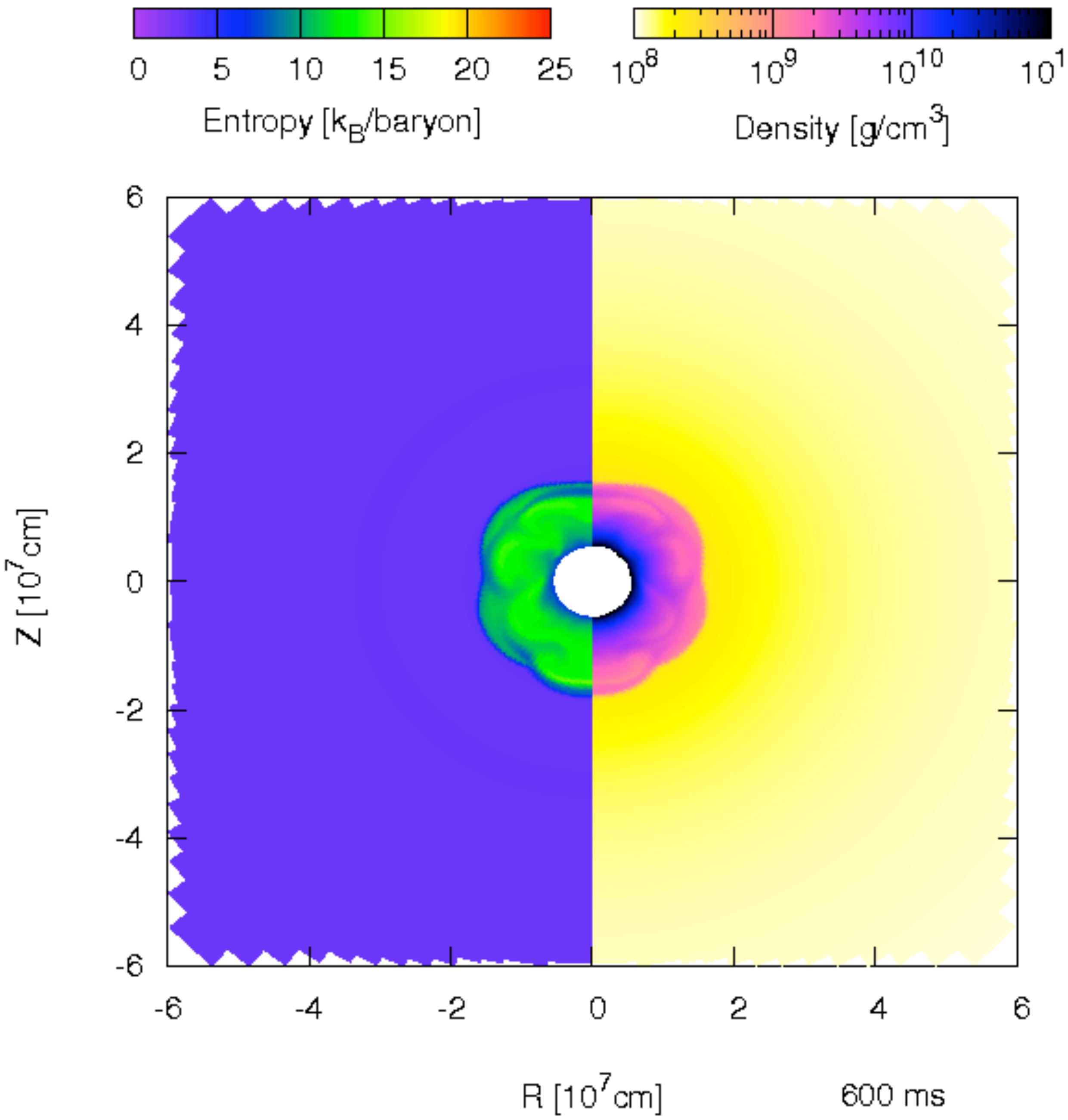

$L_\nu = 5.5 \times 10^{52}$ erg/s

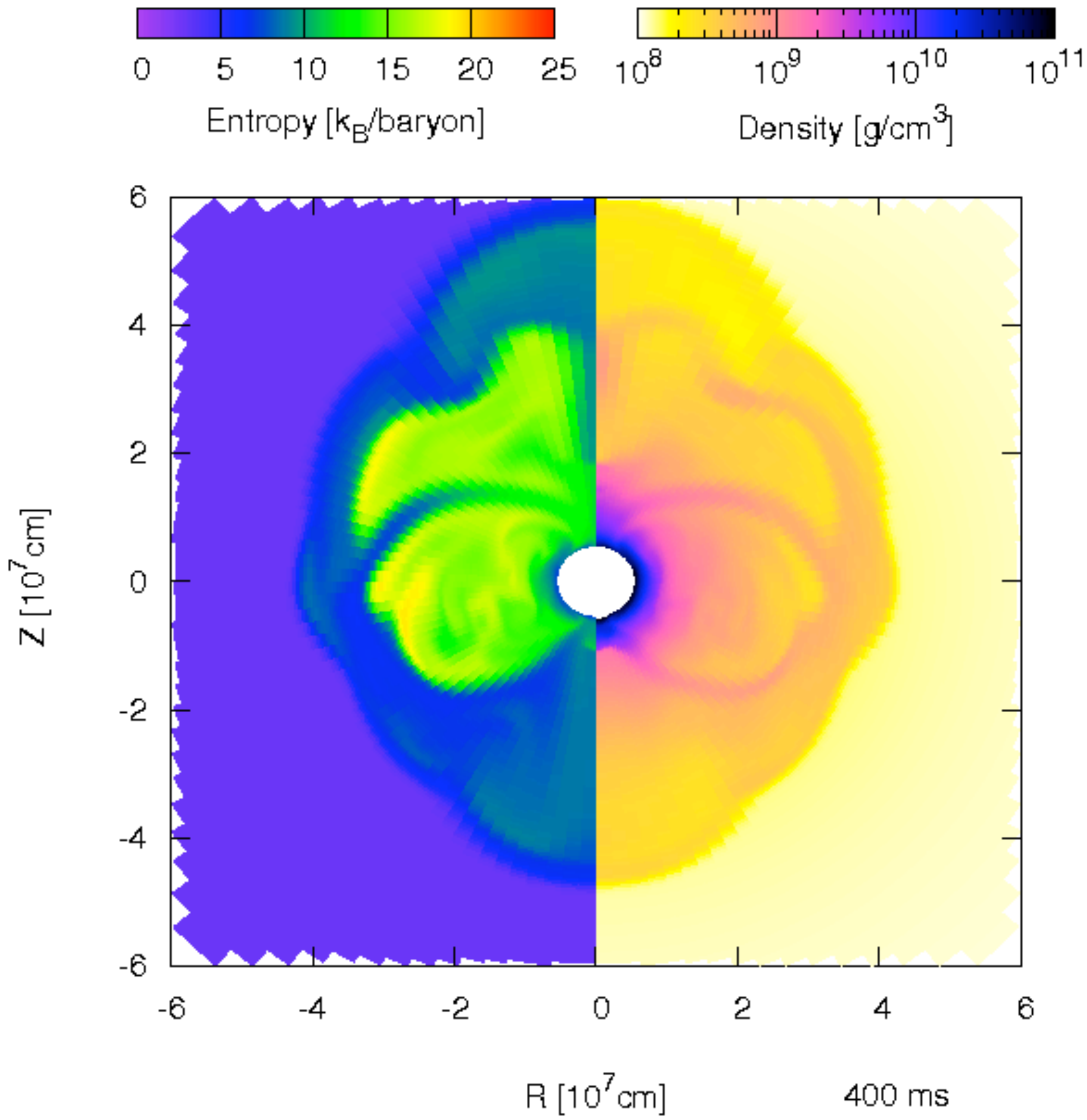

$L_\nu = 6.0 \times 10^{52}$ erg/s

Amplitude of shock surface perturbation exponentially grows during ~100 ms

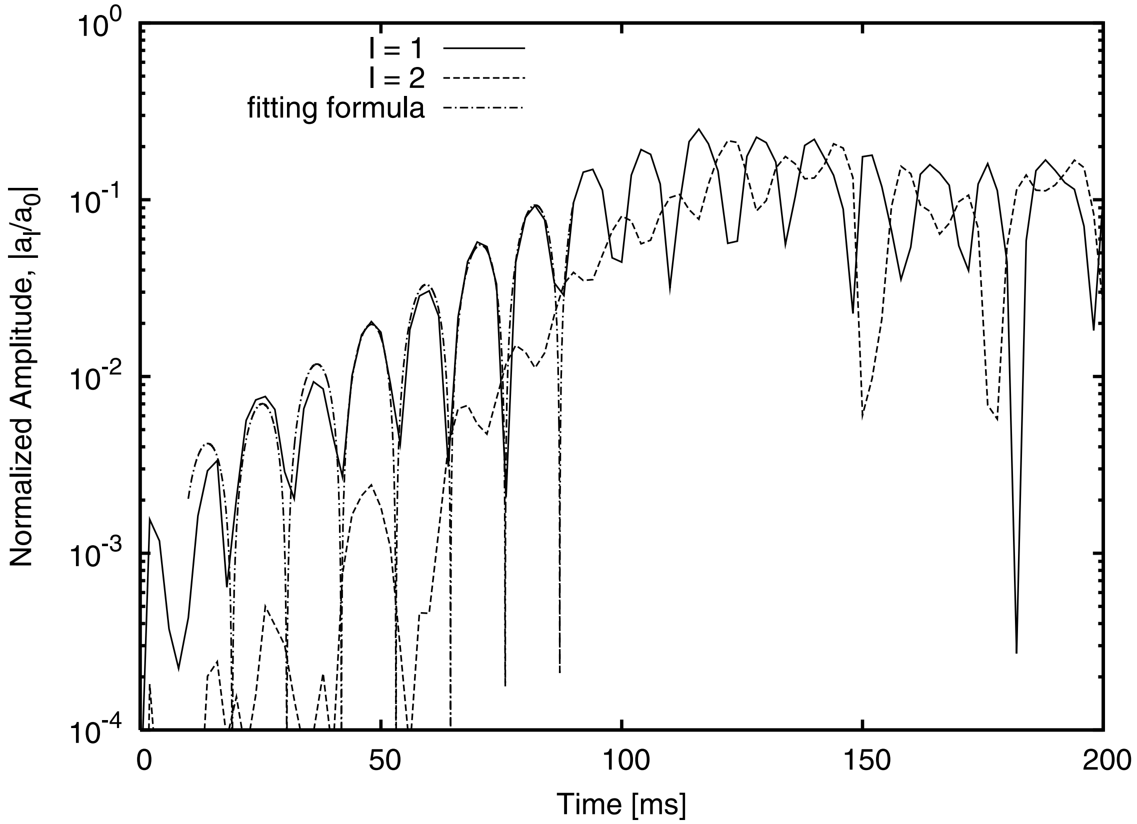

FIG. 5.—Temporal evolutions of the normalized amplitudes of the $l = 1, 2$ modes for the model with $L_\nu = 5.5 \times 10^{52}$ ergs s^{-1}. The dot-dashed line represents the fitting in the linear phase.

TABLE 1

KEY VARIABLES IN SASI

L_ν (10^{52} ergs s^{-1})	γ (s^{-1})	ω (s^{-1})	$R_{s,\rm equil}$ (10^5 cm)	w_s (10^5 cm)	$\omega_{\rm adv}$ (s^{-1})	$\omega_{\rm snd}$ (s^{-1})	$\omega_{\rm cyc}$ (s^{-1})
3.0	42.4	915	66.9	30.9	1098	5867	925
5.5	45.7	277	128	79.2	262	1832	229
6.0	38.3	188	144	93.5	207	1497	181
6.5	35.6	143	167	114	159	1199	141

NOTES.—L_ν represents the model luminosities. The growth rate and the oscillation frequency, denoted as γ and ω, respectively, are obtained by least-squares fitting to the numerical results in the linear regime. The quantity $R_{s,\rm equil}$ is the initial shock radius, and w_s is the distance between the shock radius and the neutrinosphere; $w_s = R_{s,\rm equil} - r_\nu$. The frequencies associated with the advection and the sound propagation between the shock and the neutrinosphere are denoted as $\omega_{\rm adv}$ and $\omega_{\rm snd}$, respectively, and are defined as $\omega_{\rm adv} = 2\pi/\int_{r_\nu}^{R_s}(1/v_r)\,dr$ and $\omega_{\rm snd} = 2\pi/\int_{r_\nu}^{R_s}(1/c_s)\,dr$, respectively. They are evaluated numerically for the initial conditions. The characteristic frequency of SASI is given by the cycle frequency, $\omega_{\rm cyc} = 2\pi/[\int_{r_\nu}^{R_s}(1/v_r)\,dr + \int_{r_\nu}^{R_s}(1/c_s)\,dr]$. See text for more details.

(Ohnishi et al. 2006)

Lower modes are dominated even if the simulation starts with random moulti-mode perturbations

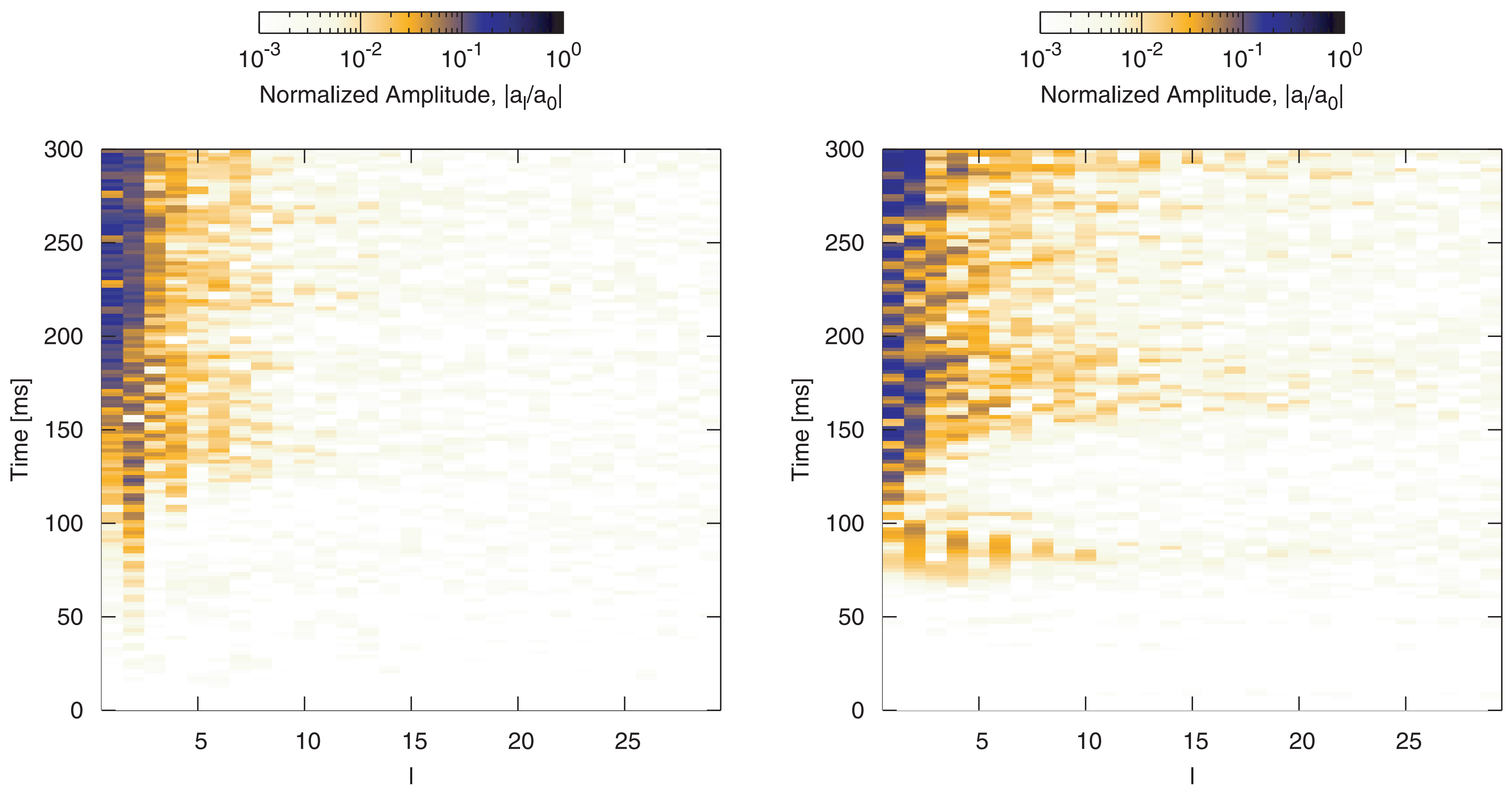

FIG. 6.—Temporal evolutions of the spectra in the spherical harmonics decomposition for the models with $L_\nu = 3.0 \times 10^{52}$ ergs s^{-1} (*left*) and $L_\nu = 5.5 \times 10^{52}$ ergs s^{-1} (*right*). The random multimode velocity perturbations are initially added.

SASI may enhance inelastic scattering due to Helium production at shock front

- incoherent scattering by neuclei ($\nu + (A,Z) \rightarrow \nu + (A,Z)^*$)

$$
\begin{aligned}
Q_{\mathrm{incoh}} = \frac{\rho X_{\mathrm{A}}}{m_{\mathrm{B}}} \frac{31.6\mathrm{MeV}}{(r/10^7\mathrm{cm})^2} \Bigg[& \frac{L_{\nu_e}}{10^{52}\mathrm{erg/s}} \left(\frac{5\mathrm{MeV}}{T_{\nu_e}}\right) \frac{A^{-1}\langle \sigma^+_{\nu_e} E_{\nu_e} + \sigma^0_{\nu_e} E^{\mathrm{A}}_{\mathrm{ex}} \rangle_{T_{\nu_e}}}{10^{-40}\mathrm{cm}^2\mathrm{MeV}} \\
& \frac{L_{\bar{\nu}_e}}{10^{52}\mathrm{erg/s}} \left(\frac{5\mathrm{MeV}}{T_{\bar{\nu}_e}}\right) \frac{A^{-1}\langle \sigma^-_{\bar{\nu}_e} E_{\nu_e} + \sigma^0_{\bar{\nu}_e} E^{\mathrm{A}}_{\mathrm{ex}} \rangle_{T_{\bar{\nu}_e}}}{10^{-40}\mathrm{cm}^2\mathrm{MeV}} \\
& \frac{L_{\nu_\mu}}{10^{52}\mathrm{erg/s}} \left(\frac{10\mathrm{MeV}}{T_{\nu_\mu}}\right) \frac{A^{-1}\langle \sigma^0_{\nu_\mu} E^{\mathrm{A}}_{\mathrm{ex}} + \sigma^0_{\bar{\nu}_\mu} E^{\mathrm{A}}_{\mathrm{ex}} \rangle_{T_{\nu_\mu}}}{10^{-40}\mathrm{cm}^2\mathrm{MeV}} \Bigg]
\end{aligned}
$$

- fitting formula of neutral-current cross section

$$A^{-1}\langle \sigma^0_{\nu} E^{\mathrm{A}}_{\mathrm{ex}} + \sigma^0_{\bar{\nu}} E^{\mathrm{A}}_{\mathrm{ex}} \rangle_{T_\nu} = \alpha \left[\frac{T - T_0}{10\mathrm{MeV}}\right]^\beta$$

- parameters of neutral-current cross section for ^{4}He

$$\alpha = 1.24 \cdot 10^{-40}\ \mathrm{MeV\ cm}^2,\ \beta = 3.82,\ T_0 = 2.54\ \mathrm{MeV}$$

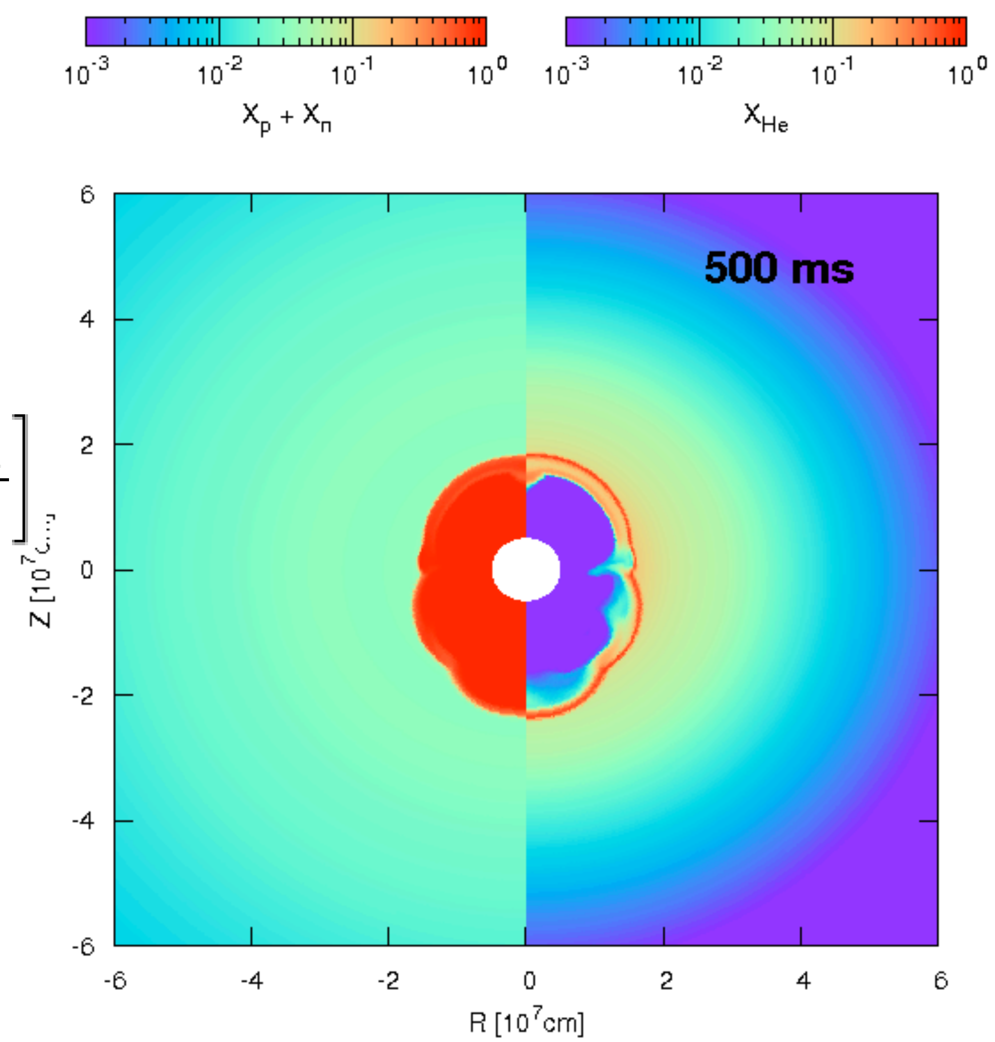

Inelastic scattering can be estimated by a fitting formula (Haxton 1988)

(L_ν = 5.9x10^{52} erg/s)

Explosion is failed with incoherent scattering, but succeeded with an additional artificial factor

L_ν = 5.9x10^{52} erg/s

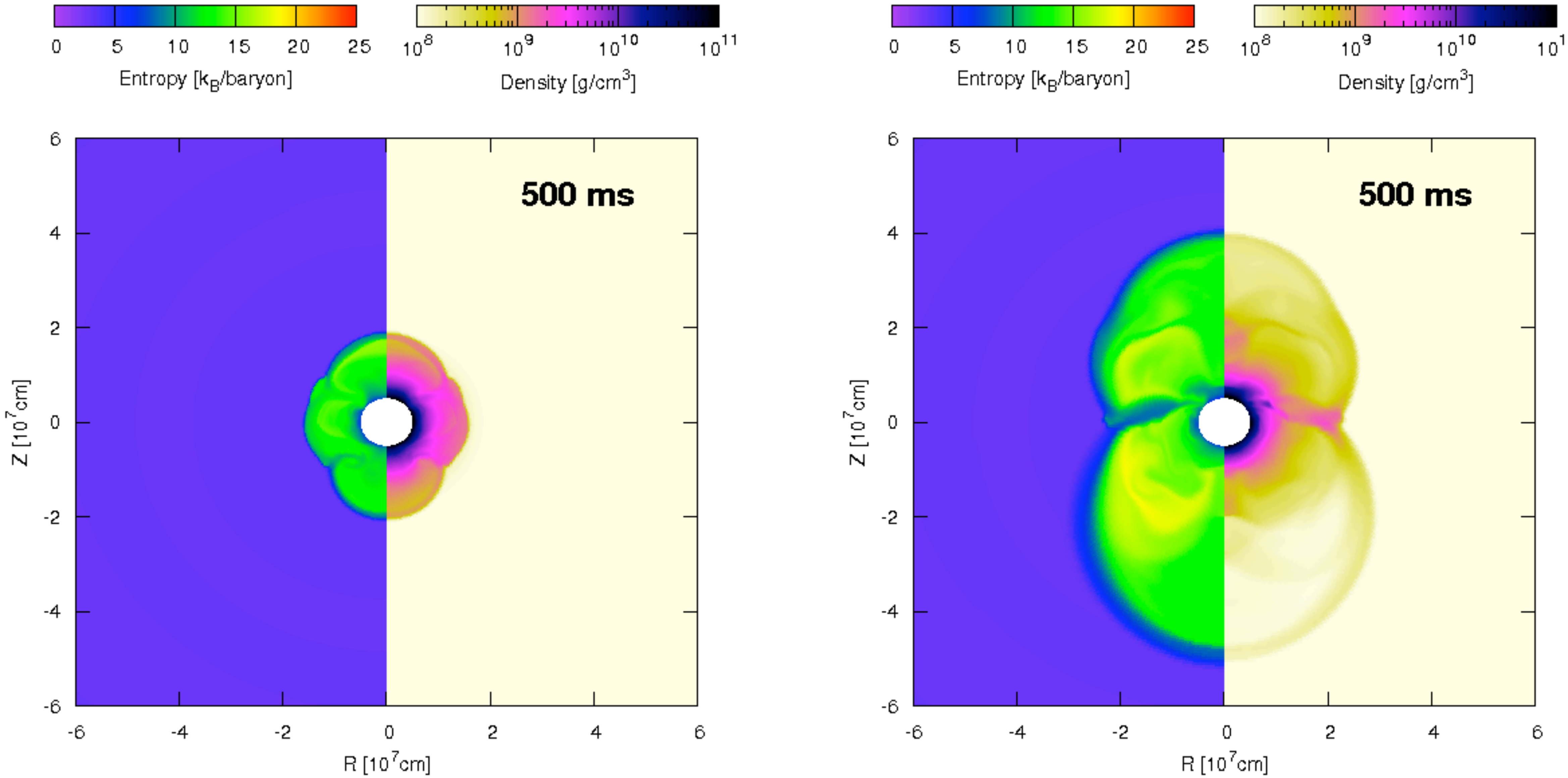

x1 incoherent scattering **x10 incoherent scattering**

(Ohnishi et al. 2007)

Many simulations indicate that the inelastic scattering does not contribute so much to the successful explosion

TABLE 1
MODEL PARAMETERS

Model	L_{ν_e} (10^{52} ergs s^{-1})	Q_{inel} (eq. [6])	$\delta v_r / v_r^{1D}$ (%)	$T_{\nu_{\mu,\tau}}$ (MeV)	Shock Revival
L59I0...........	5.9	–	1	10	X
L59I1...........	5.9	1	1	10	X
L59I3...........	5.9	3	1	10	X
L59I10..........	5.9	10	1	10	◯
L59I30..........	5.9	30	1	10	◯
L59I0d5........	5.9	–	5	10	X
L59I1d5........	5.9	1	5	10	X
L59I3d5........	5.9	3	5	10	◯
L59I0d10......	5.9	–	10	10	◯
L59T15.........	5.9	1	1	15	X
L59T20.........	5.9	1	1	20	X
L59T25.........	5.9	1	1	25	◯
L58I0...........	5.8	–	1	10	X
L58I1...........	5.8	1	1	10	X
L58I5...........	5.8	5	1	10	X
L58I10..........	5.8	10	1	10	◯
L58I15..........	5.8	15	1	10	X
L58I20..........	5.8	20	1	10	X
L58I30..........	5.8	30	1	10	X
L58I40..........	5.8	40	1	10	X
L58I50..........	5.8	50	1	10	◯
L58I100........	5.8	100	1	10	◯
L57I0...........	5.7	–	1	10	X
L57I1...........	5.7	1	1	10	X
L57I10..........	5.7	10	1	10	X
L57I30..........	5.7	30	1	10	X
L57I100........	5.7	100	1	10	◯
L55I0...........	5.5	–	1	10	X
L55I1...........	5.5	1	1	10	X
L55I10..........	5.5	10	1	10	X
L55I30..........	5.5	30	1	10	X
L55I100........	5.5	100	1	10	X

NOTES.—The variable L_{ν_e} represents the luminosity of the electron-type neutrino. For Q_{inel}, only the multiplicative factor is given. The term $\delta v_r / v_r^{1D}$ denotes the initial relative amplitude of the velocity perturbation. The variable $T_{\nu_{\mu,\tau}}$ is the temperature of mu and tau neutrinos. The "successful shock revival" is defined as a continuous increase of the shock radius by ~500 ms.

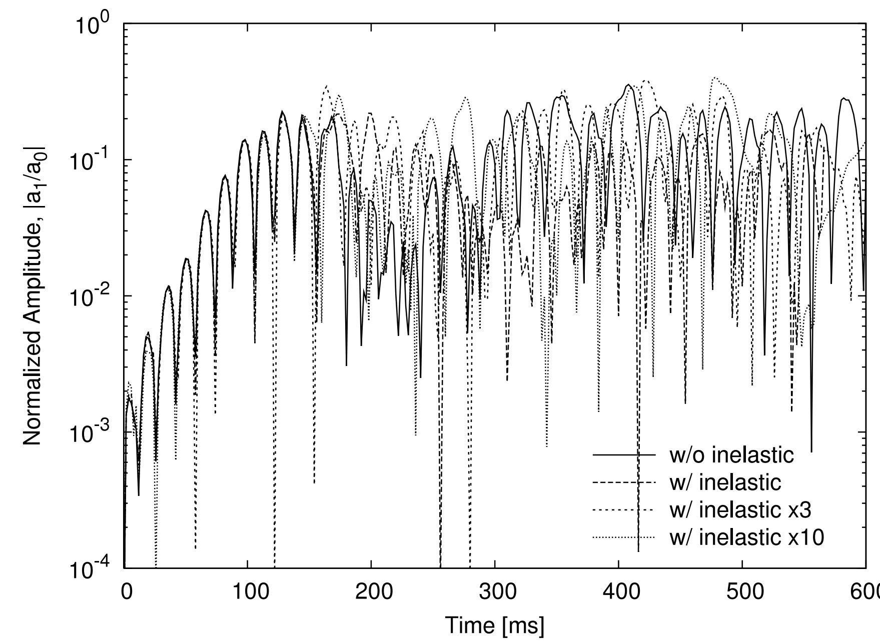

FIG. 3.—Temporal evolution of the normalized amplitudes of the $\ell = 1$ mode in the spherical harmonic decompositions for models L59I0, L59I1, L59I3, and L59I10. See the text for details.

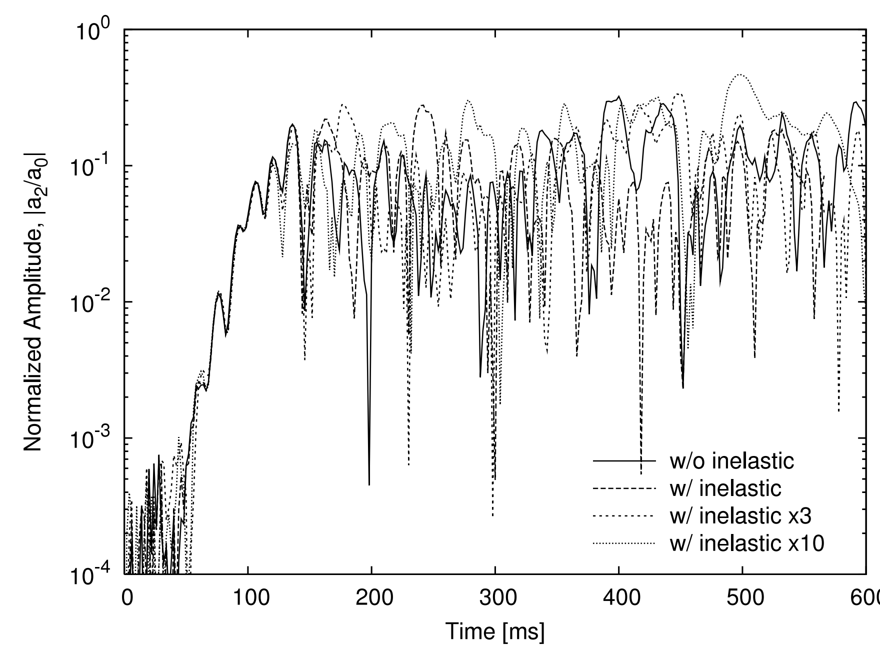

FIG. 4.—Same as Fig. 3, but for $\ell = 2$.

Acoustic power generated in the inner core may drive an explosion

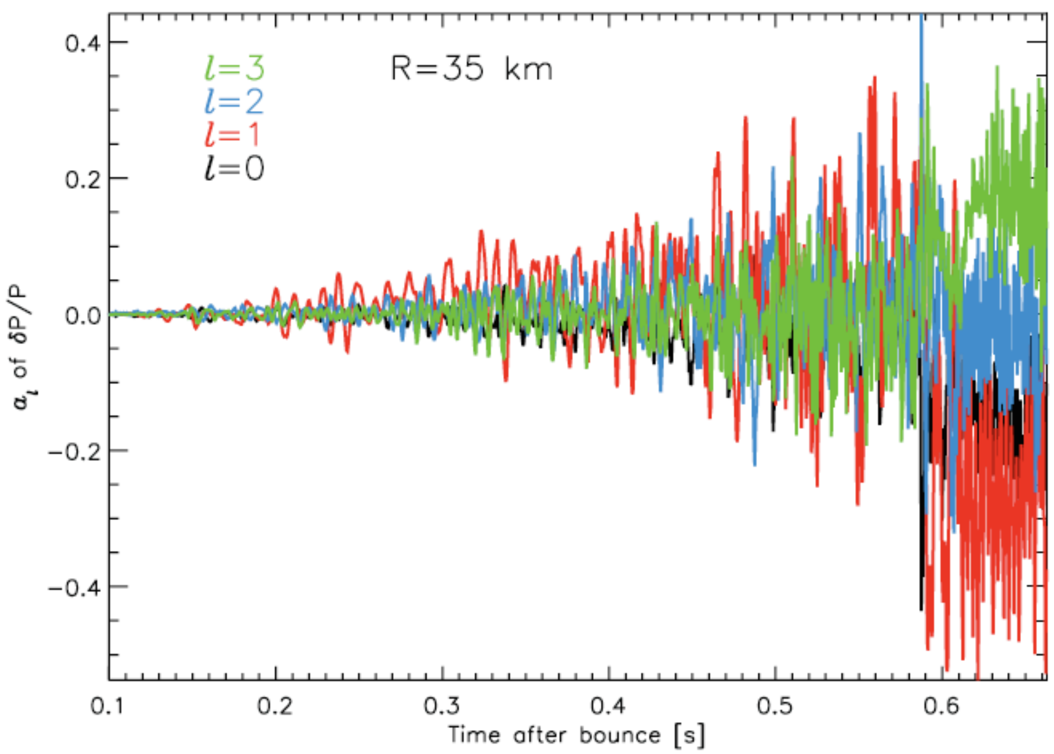

FIG. 7.—Time evolution of the spherical harmonic coefficients for the fractional pressure variation for modes $\ell = 0$ (*black*), 1 (*red*), 2 (*blue*), and 3 (*green*) at a radius $R = 35$ km, given by $a_\ell = 2\pi \int_0^\pi d\theta \sin\theta Y_\ell^0(\theta)[P(R,\ \theta) - \langle P(R,\ \theta)\rangle_\theta]/\langle P(R,\ \theta)\rangle_\theta$. Notice that despite the fact that the $\ell = 1$ mode looms large, the $\ell = 2$ and 3 modes are also in evidence. The $\ell = 2$ (harmonic) mode will result in a distinctive signature in gravitational radiation detectors, initially at a frequency near ~675 Hz. This frequency is likely to be different (higher) when general relativity is included (Ferrari et al. 2003).

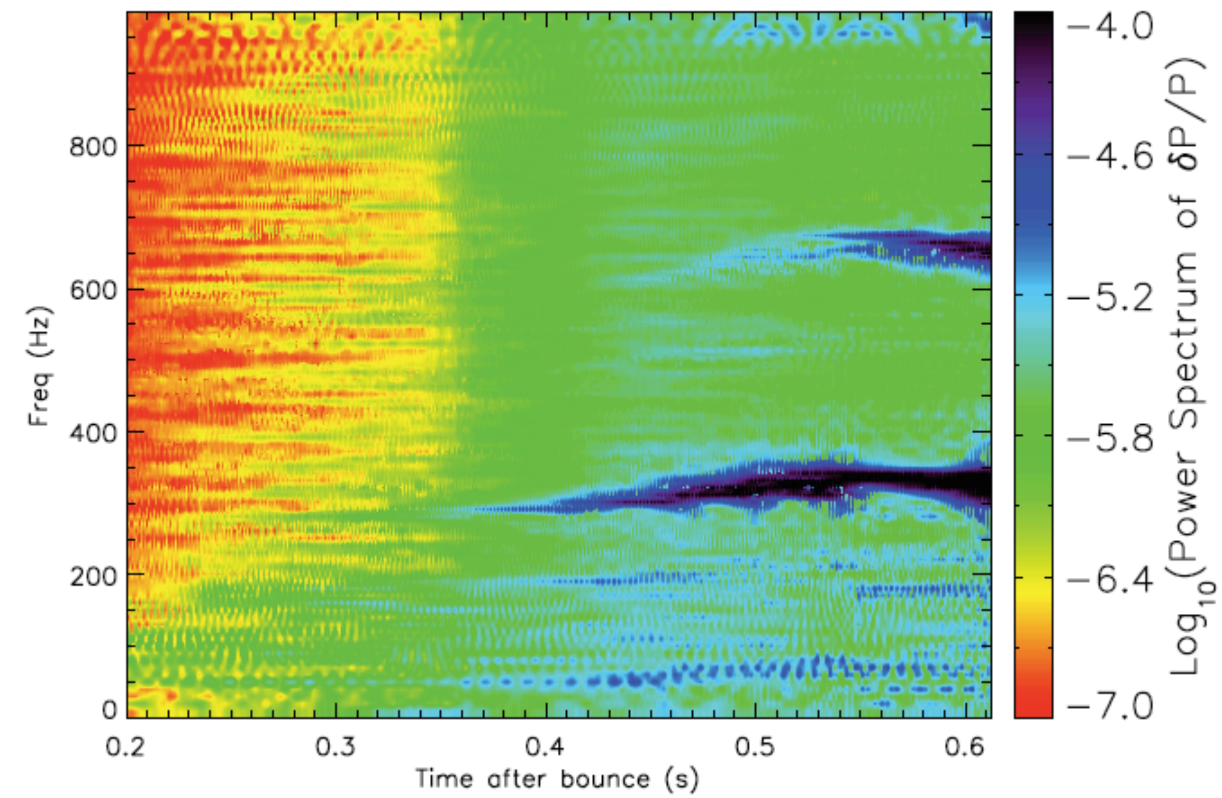

FIG. 9.—Color scale of the angle-averaged power spectrum of the fractional pressure variation $[P(R,\ \theta) - \langle P(R,\ \theta)\rangle_\theta]/\langle P(R,\ \theta)\rangle_\theta$ at a radius $R = 30$ km, as a function of time and frequency. For each time t, a power spectrum is calculated from a sample of time snapshots covering $t \pm 50$ ms, at a resolution of 0.5 ms. Note the emergence of power in the ~330 Hz (≡3 ms) g-mode, as well as the strengthening $\ell = 2$ harmonic mode near ~675 Hz at late times. The latter is of relevance for gravitational radiation emission.

(Burrows et al. 2006)

Excitation of g-mode by SASI is inefficient due to the severe impedance mismatch

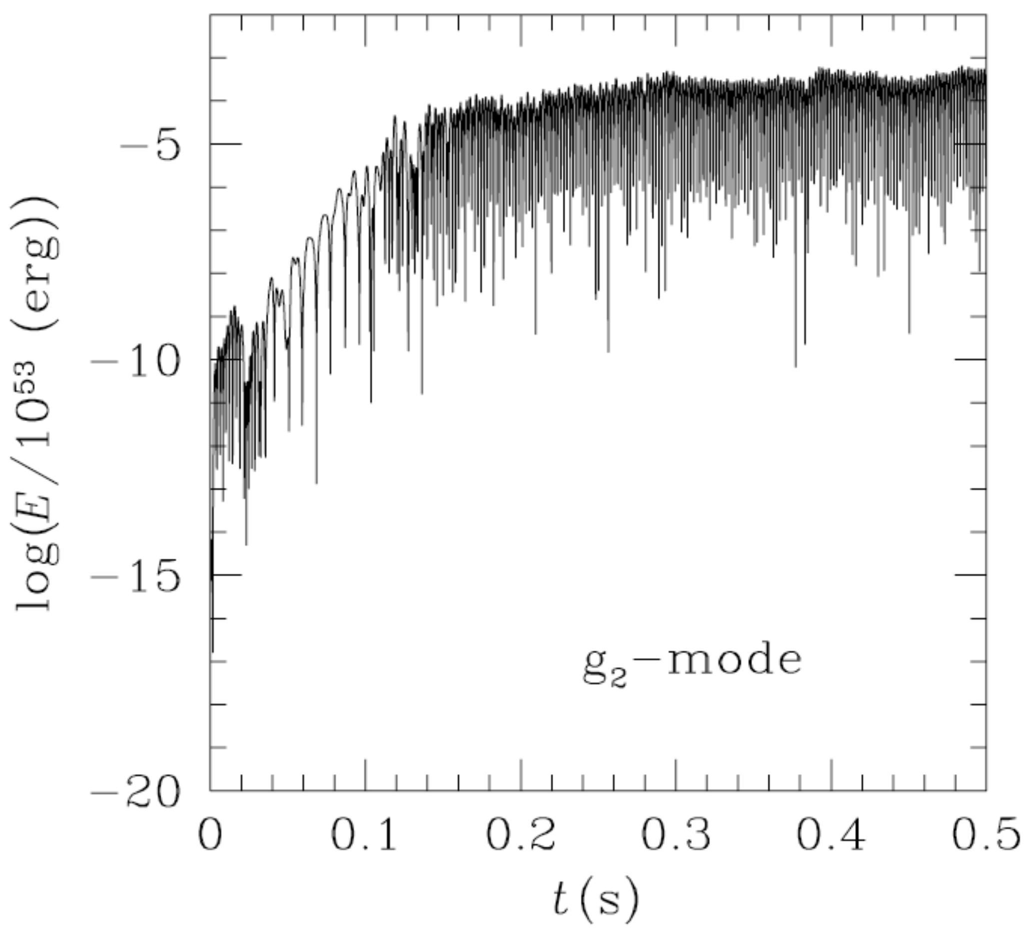

FIG. 5.—Time evolution of the mode energy for the g_2-mode with $l = 1$ for the proto−neutron star model given in Fig. 2.

TABLE 1

KEY QUANTITIES FOR g-MODES IN THE PROTO−NEUTRON STAR

l	Mode	$\bar{\omega}$	ν (Hz)	E (10^{53} ergs)	a ($\times 10^{-3}$)	b ($\times 10^{-3}$)
1....................	g_1^s	2.92	499	5.70	3.50	1.72
	g_2^c	1.43	245	1.30	21.3	−0.299
	g_3^s	1.03	176	1.97	1.67	−0.154
2....................	g_1^s	3.15	538	7.51	5.91	0.997
	g_2^c	2.24	383	3.15	2.02	−0.101
	g_3^s	1.72	294	7.11	1.02	0.238

(Yoshida et al. 2007)

The saturated energy is less than 10^{50} ergs even with the most efficiently excited mode (g_2-mode with l=1)

Initial conditions of Ln=3.0e52 ergs/s, Mdot=0.2398M⊙

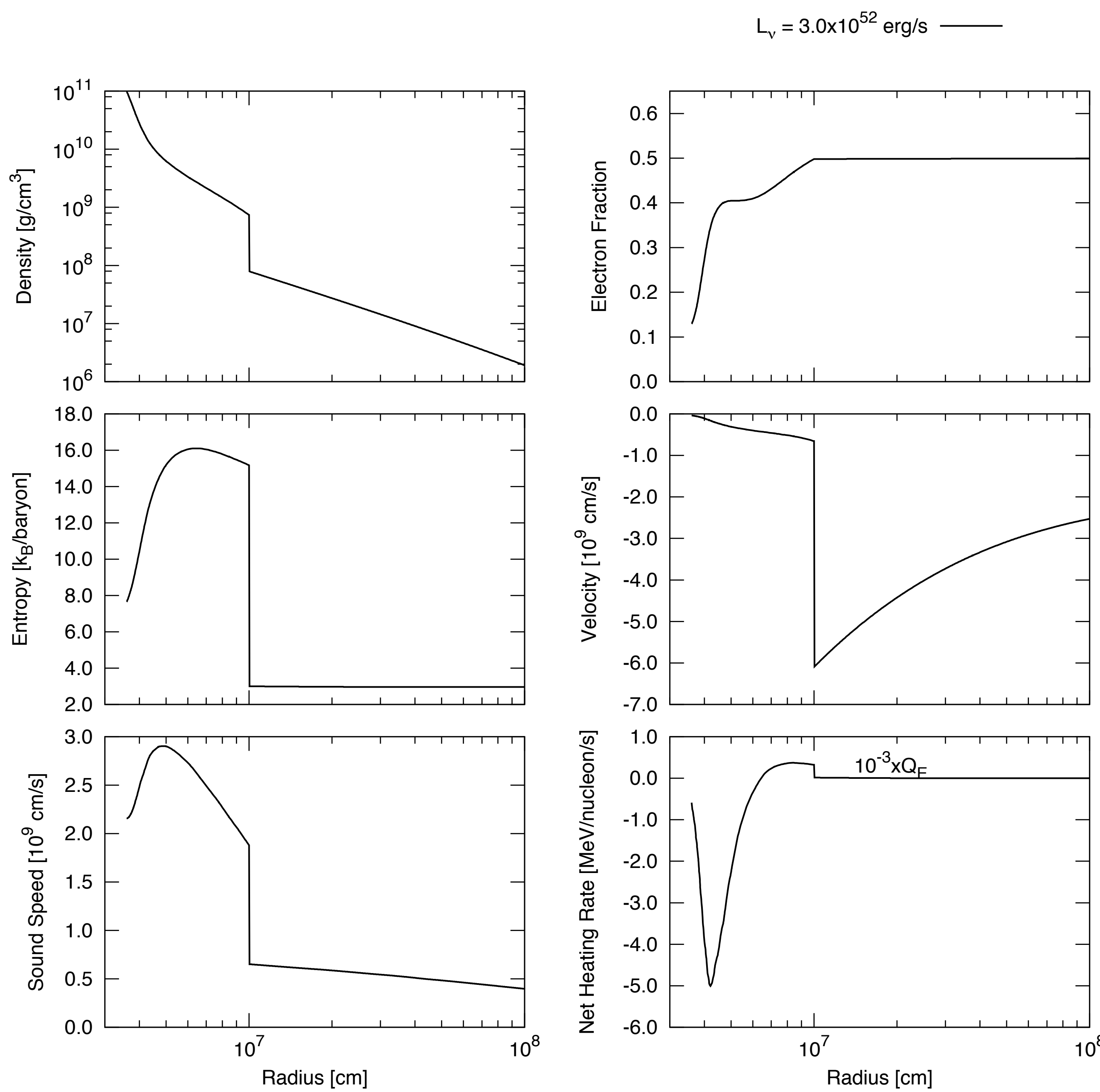

Numerical conditions

- axisymmetric
- tabulated EOS by Shen et al. (1998)
- fixed condition of the outer boundary with unperturbed state
- free outflow of the inner boundary except for the radial velocity

  $v_{r,0} = v_{r,1}(r_1^2/r_0^2)$ with constant $v_{r,1}$

  (other variables in the ghost mesh are copied with the most inner values)

- mass accretion rate and mass of the central object are fixed with

  $\dot{M} = 0.2398\, M_\odot\ \mathrm{s}^{-1}$ and $M_\mathrm{in} = 1.4\, M_\odot$

- $T_{\nu_e} = 4$ MeV and $T_{\bar{\nu}_e} = 5$ MeV

- pressure perturbation at the inner boundary with g-mode frequency

Perturbation growth in the early stage

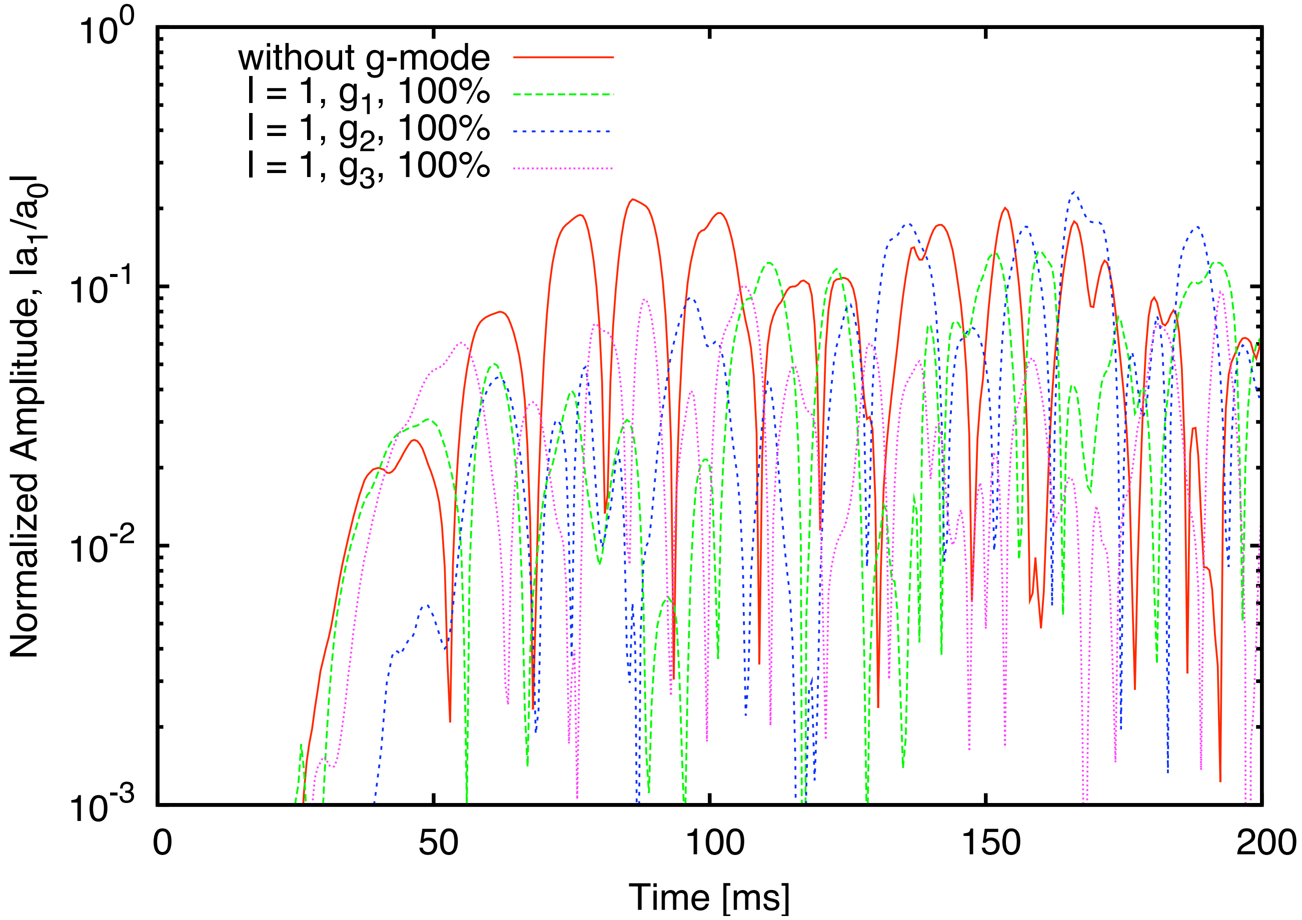

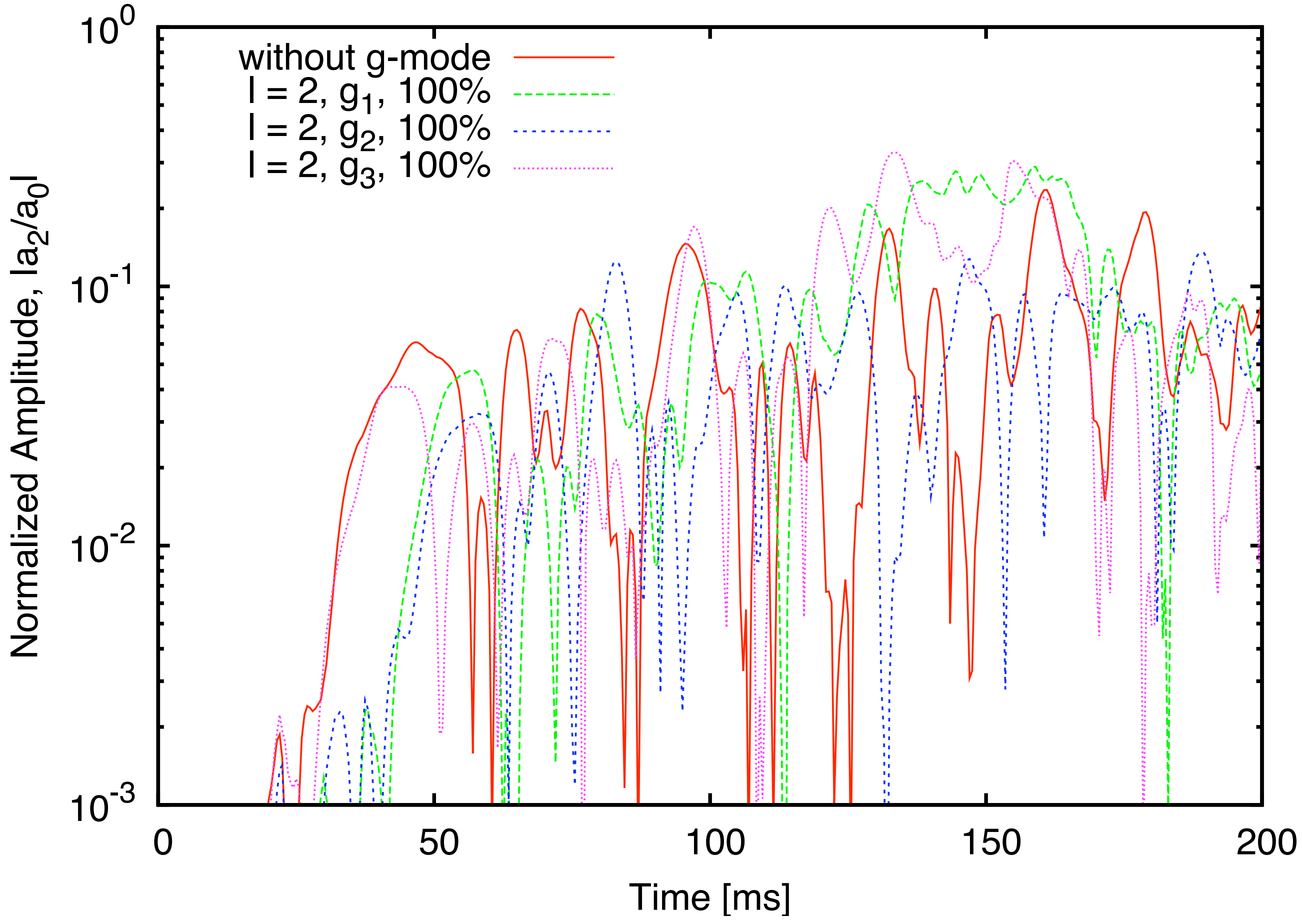

Viscous heating estimated by the artificial viscosity of ZEUS code

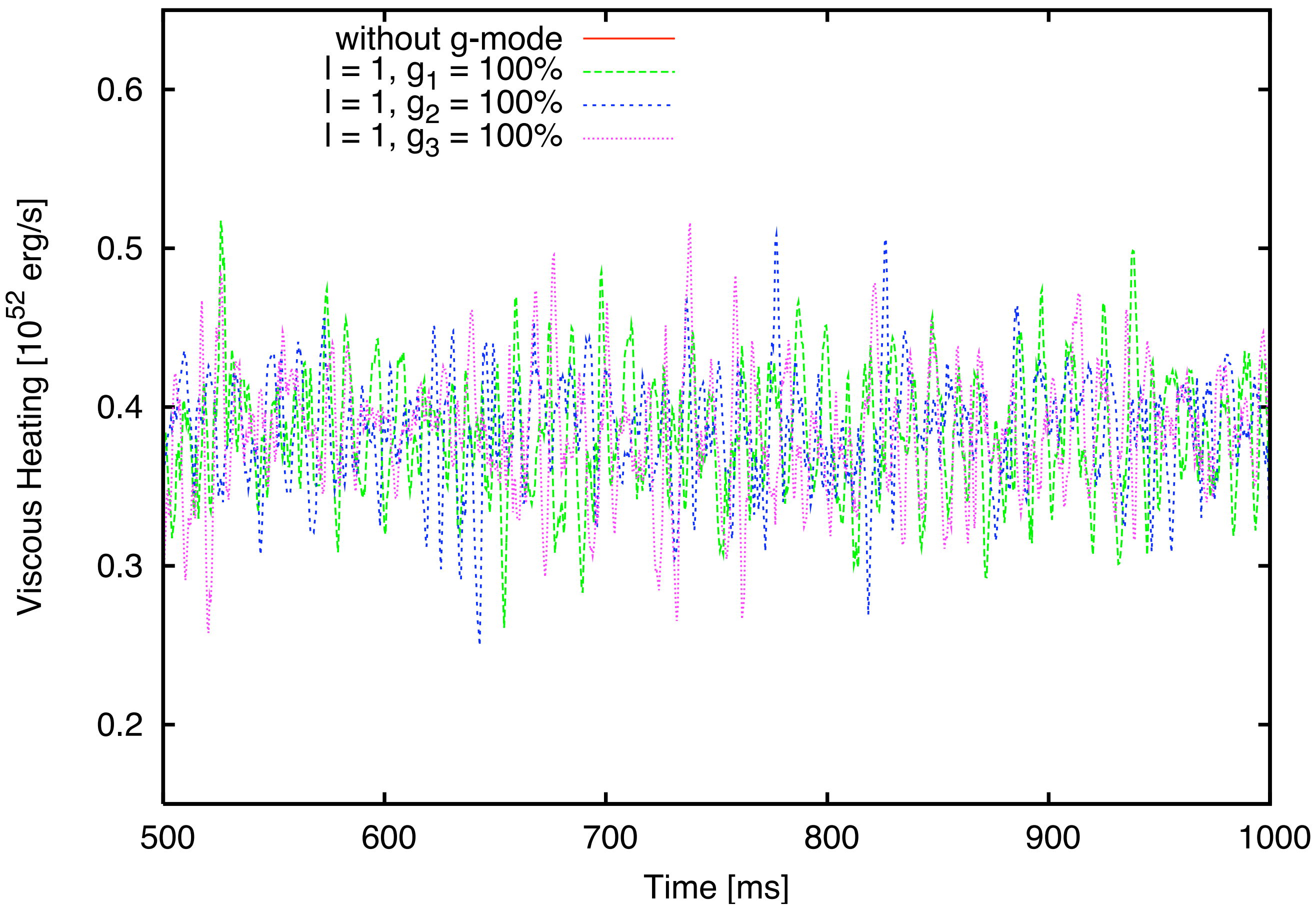

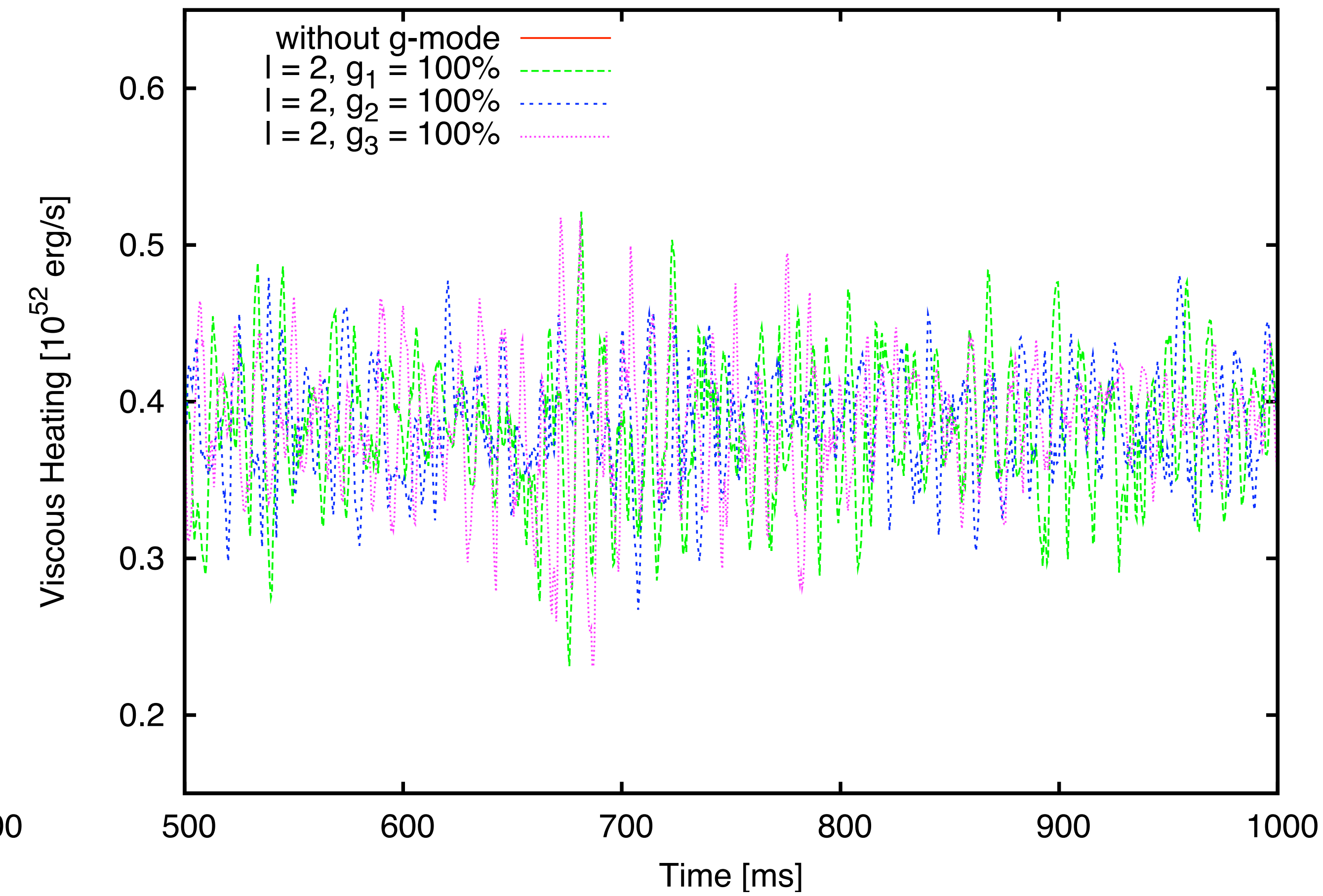

Viscous heating movies

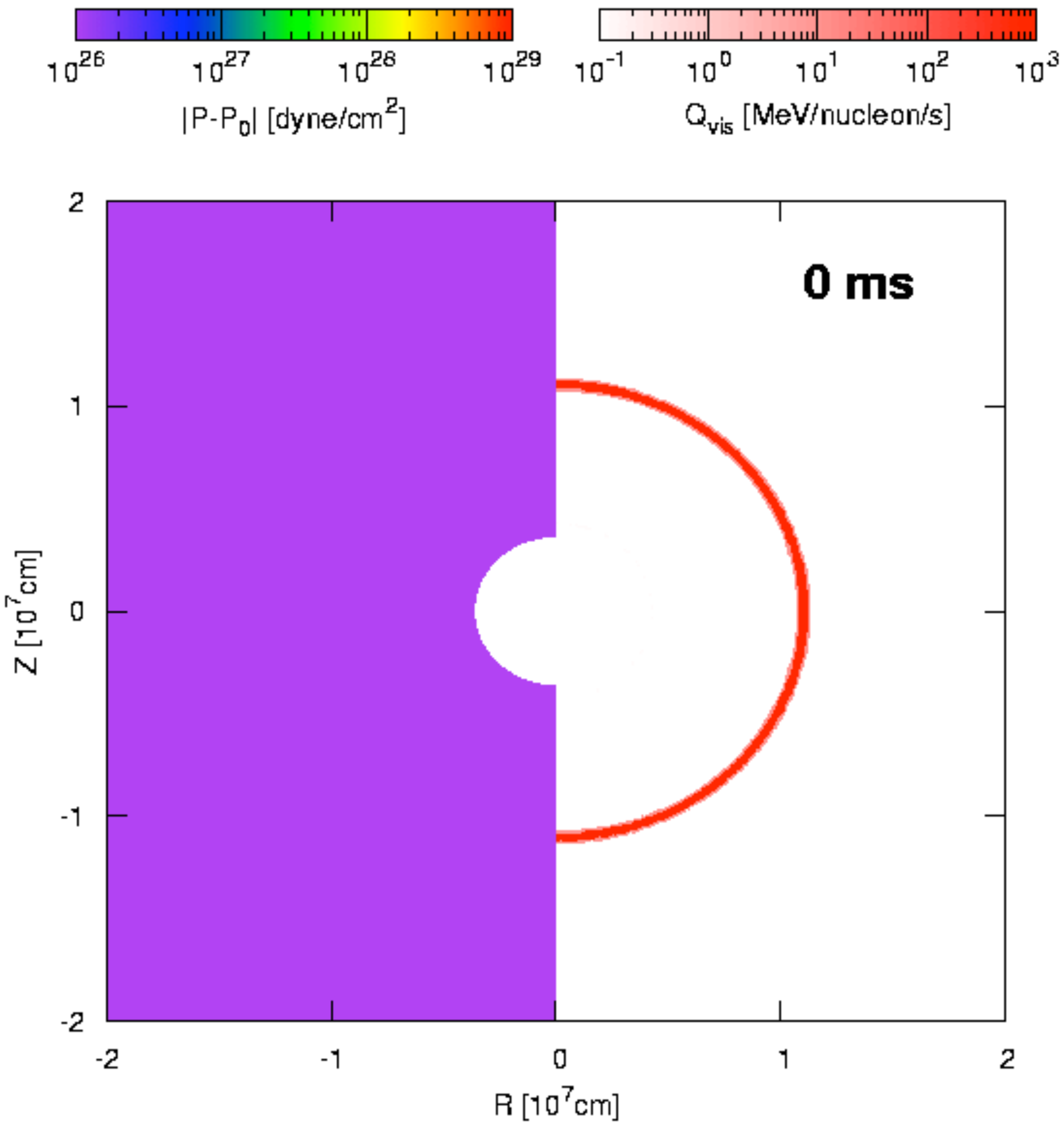

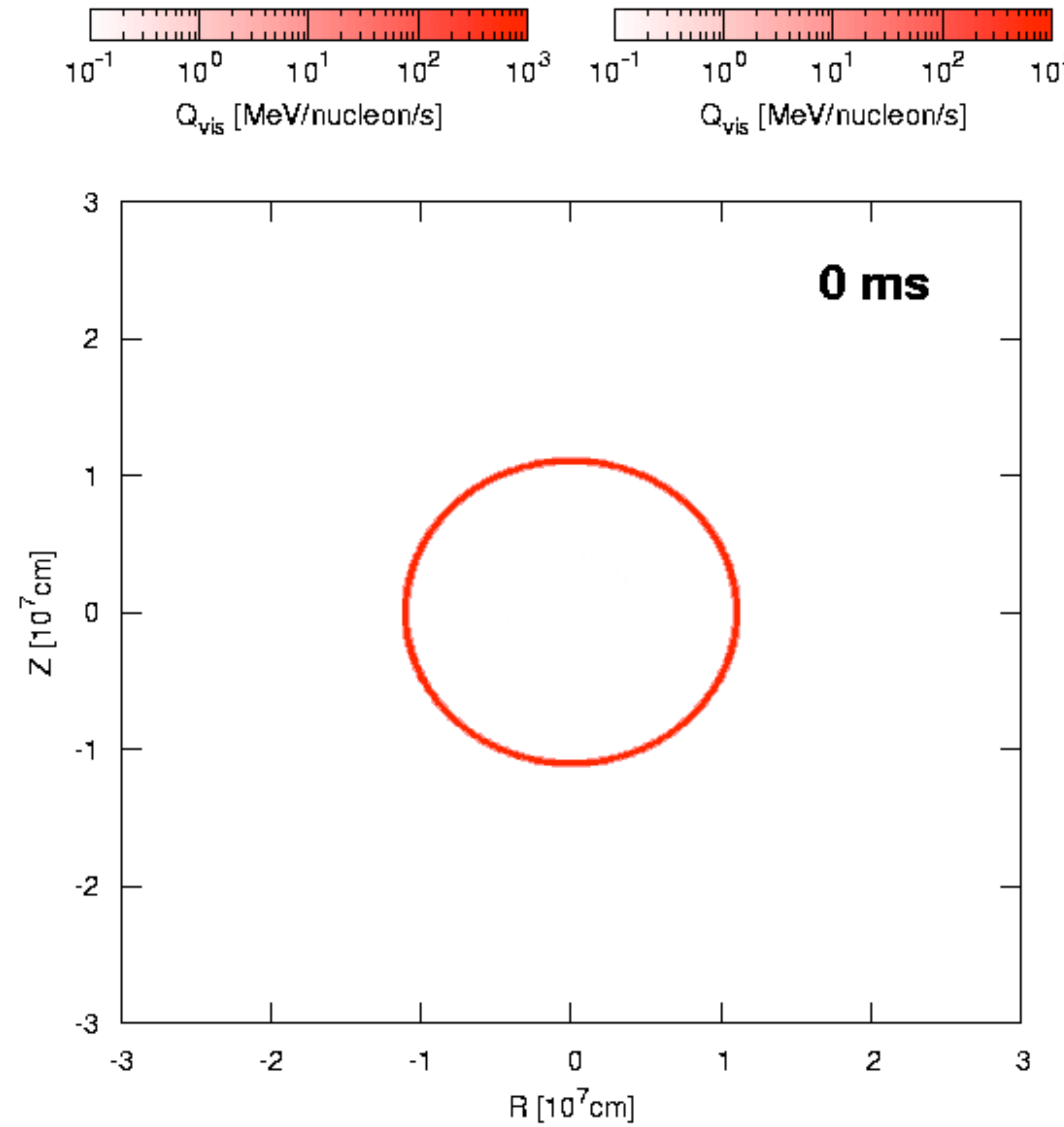

Spectral analysis of viscous heating (l=1)

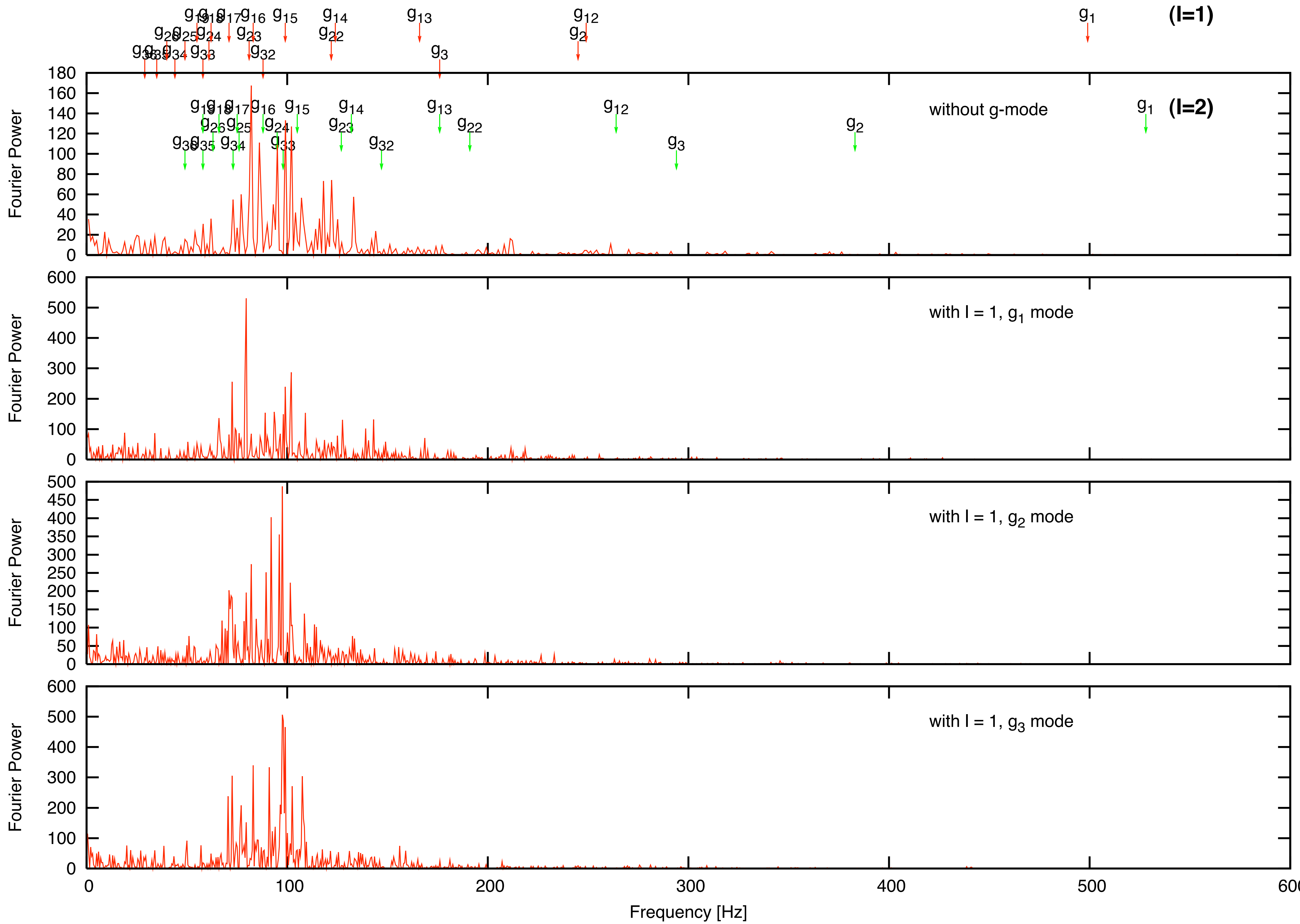

Spectral analysis of viscous heating (l=2)

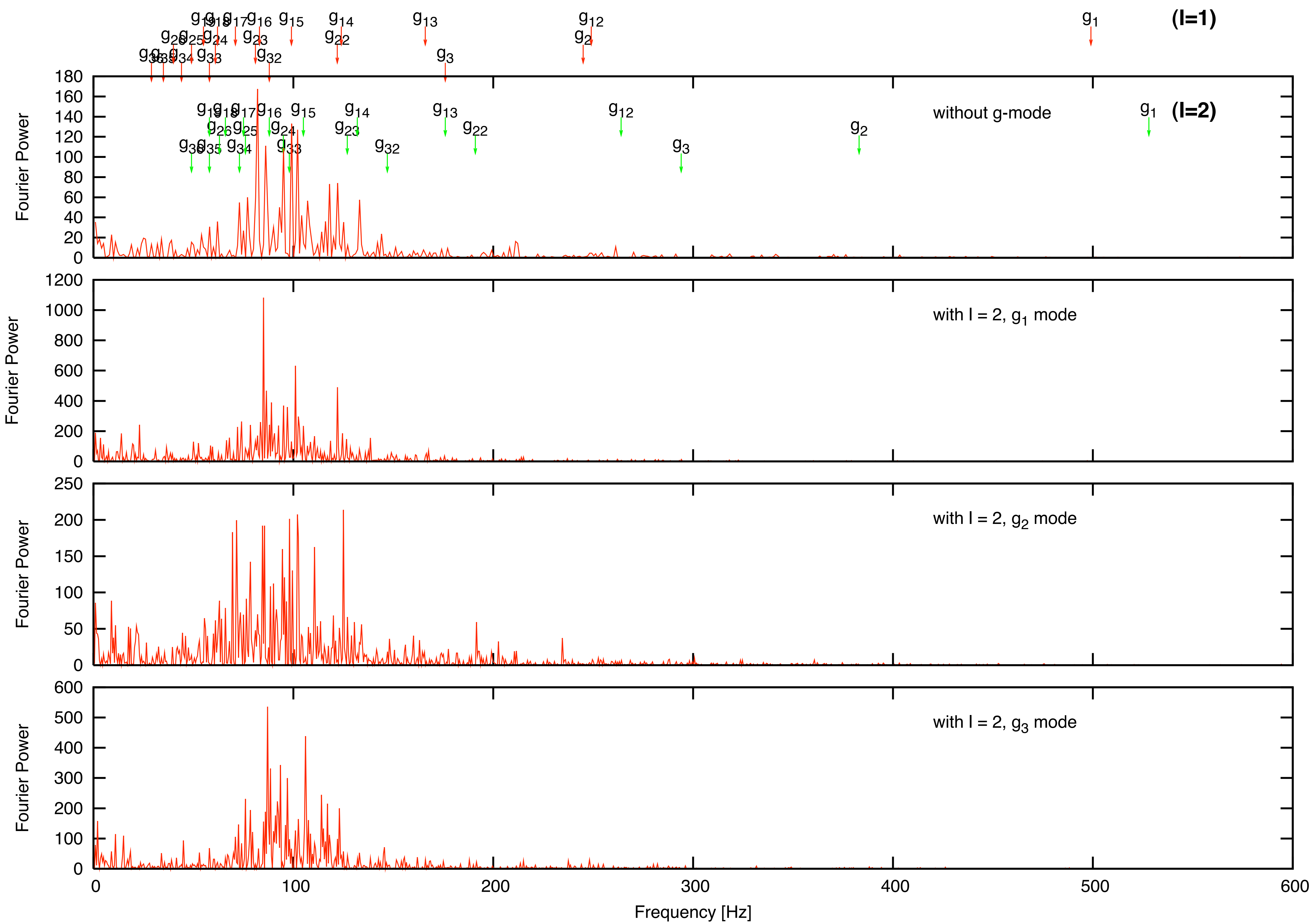

Acoustic wave propagation in the stellar atmosphere

1. ACOUSTIC CUT-OFF FREQUENCY

In the atmosphere of gravitationally bound objects (e.g. star), the density decreases with increasing height. In such circumstances, the dispersion relation of sound waves is modified. Let $-z$ be the direction of gravity. Linear perturbations, $\propto \exp\{i(\omega t - k_x x - k_z z)\}$ of the hydrodynamical equations give (sections 52 & 53 of Mihalas & Mihalas 1984)

$$\omega^4 - [\omega_{\rm a}^2 + c_{\rm s}^2(k_x^2 + k_z^2)]\omega^2 + \omega_{\rm g}^2 c_{\rm s}^2 k_x^2 = 0, \tag{1}$$

where $\omega_{\rm a}$ is acoustic cut-off frequency, and $\omega_{\rm g}$ is Brunt-Väisälä frequency. Acoustic cut-off frequency is

$$\omega_{\rm a} = \gamma g / 2c_{\rm s} = c_s / 2H, \tag{2}$$

where γ is a ratio of specific heats, g is gravity ($= GM/r^2$ for external gravity by a central star), $c_{\rm s} = dp/d\rho$ is sound speed, and H is pressure scale height. Brunt-Väisälä frequency is

$$\omega_{\rm g} = (\gamma - 1)^{1/2} g / c_{\rm s} = (\gamma - 1)^{1/2} c_{\rm s} / \gamma H \tag{3}$$

Sound waves with $\omega < \omega_a$ cannot propagate (evanescent waves). In other words, sound waves of which wavelengths $(c_{\rm s}/\omega)$ are longer than the twice of the pressure scale height are reflected because of the deformation of the wave shapes.

2. DECOMPOSITION OF ACOUSTIC WAVES

Let us consider acoustic waves that travel along with z direction in static medium ($v_z = 0$ in the unperturbed state). Owing to the longitudinal nature, acoustic waves that propagate with $+z$ direction show the positive correlation between density perturbation, $d\rho$, and velocity perturbation, v_z, while acoustic waves with $-z$ direction show the negative correlation between $d\rho$ and v_z. Then, we can define acoustic wave amplitudes of positive and negative directions:

$$s_{\pm} = v_z \pm c_{\rm s} \frac{d\rho}{\rho} \tag{4}$$

From simulation data, we can decompose acoustic perturbations into directions by this equation.

(Suzuki, private communication)

Pressure scale height for the steady-state solution of Ln=3.0e52 ergs/s

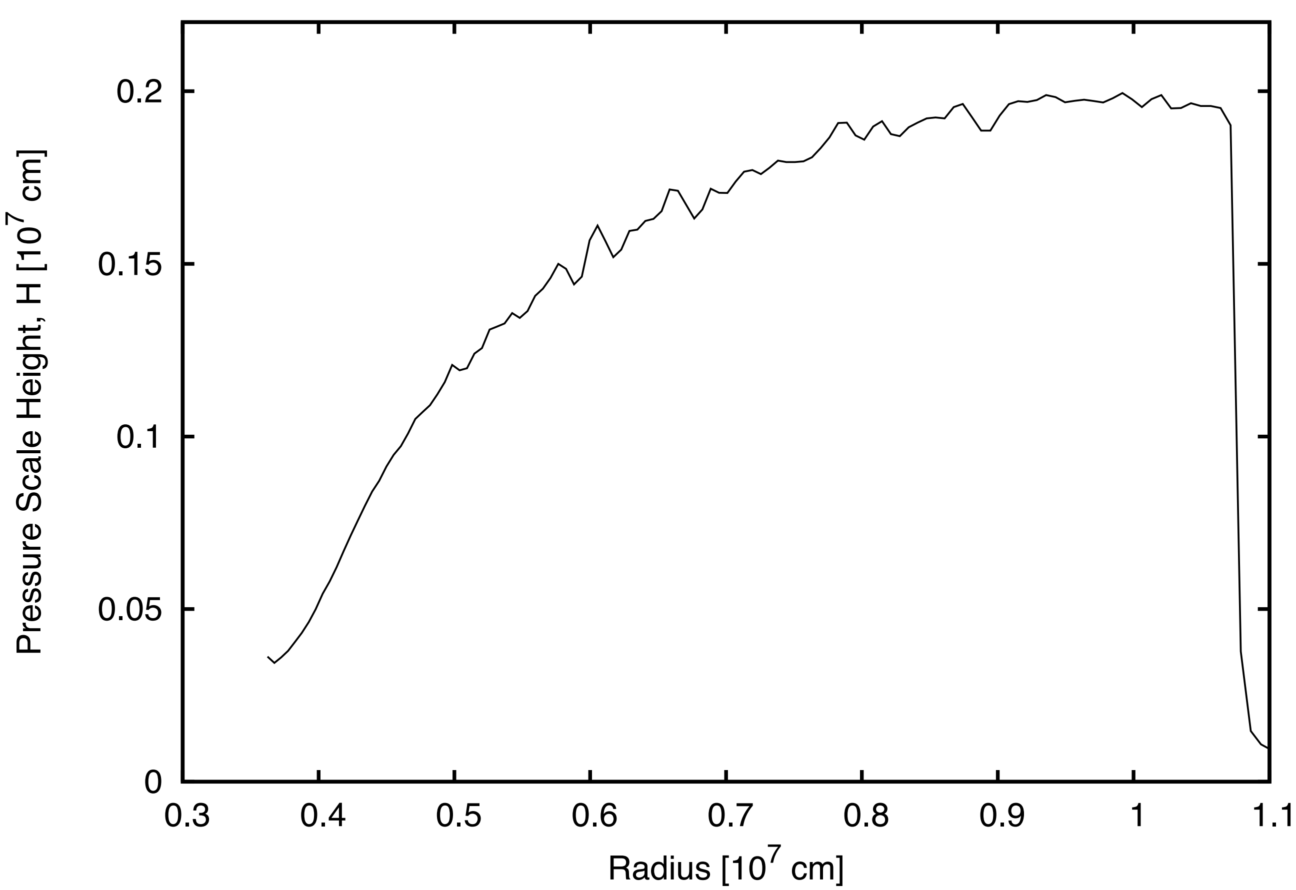

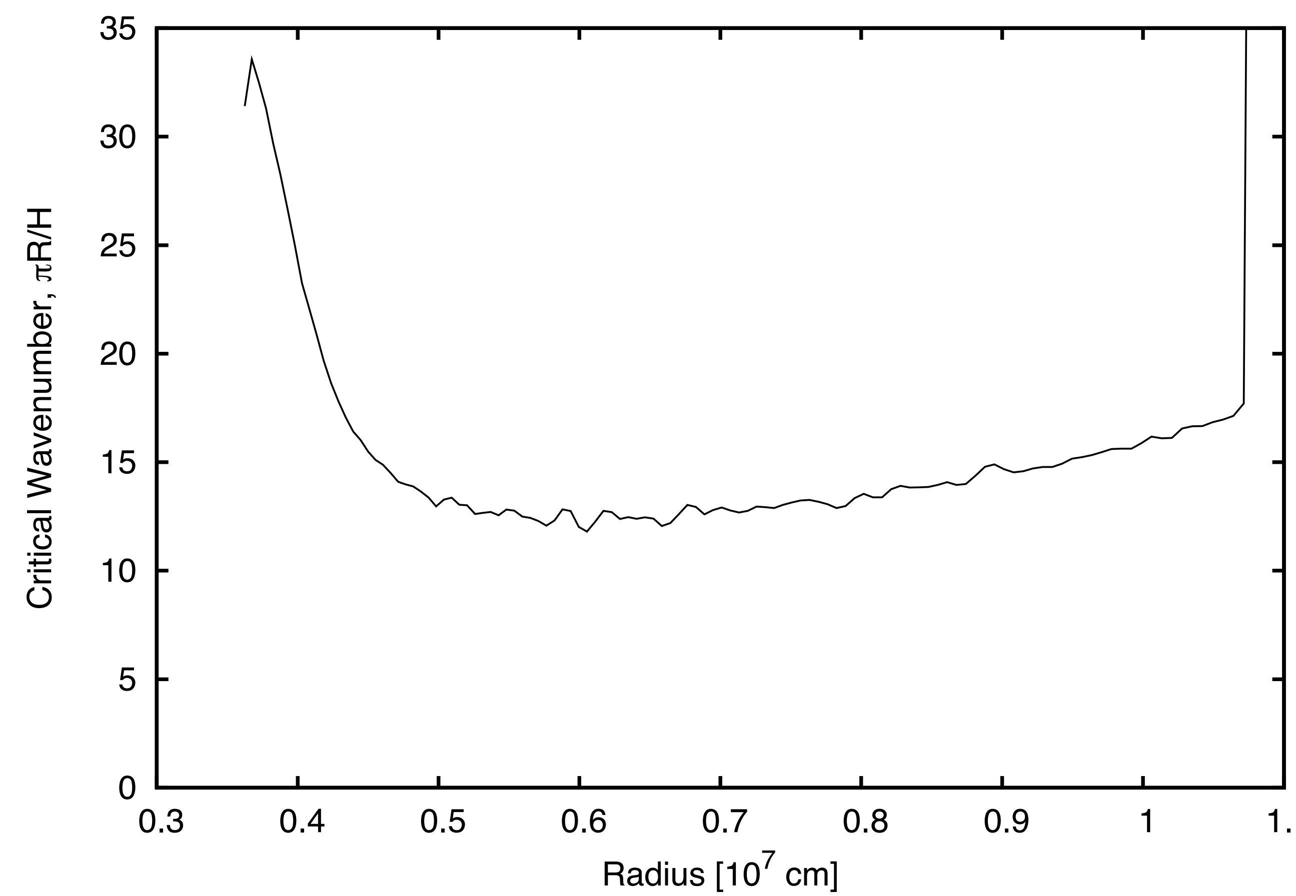

Acoustic wave propagation with random perturbation

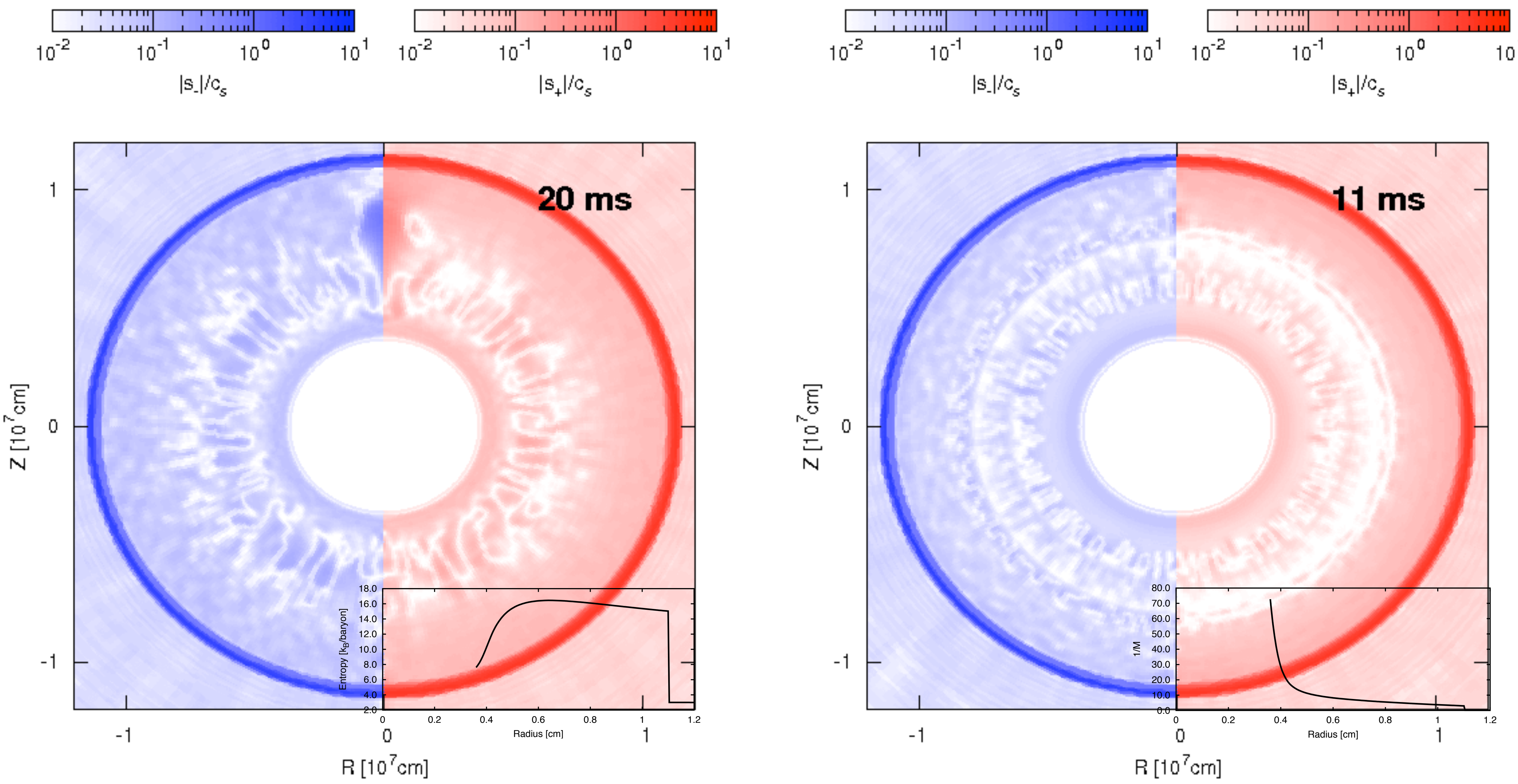

Perturbation growth in the linear phase

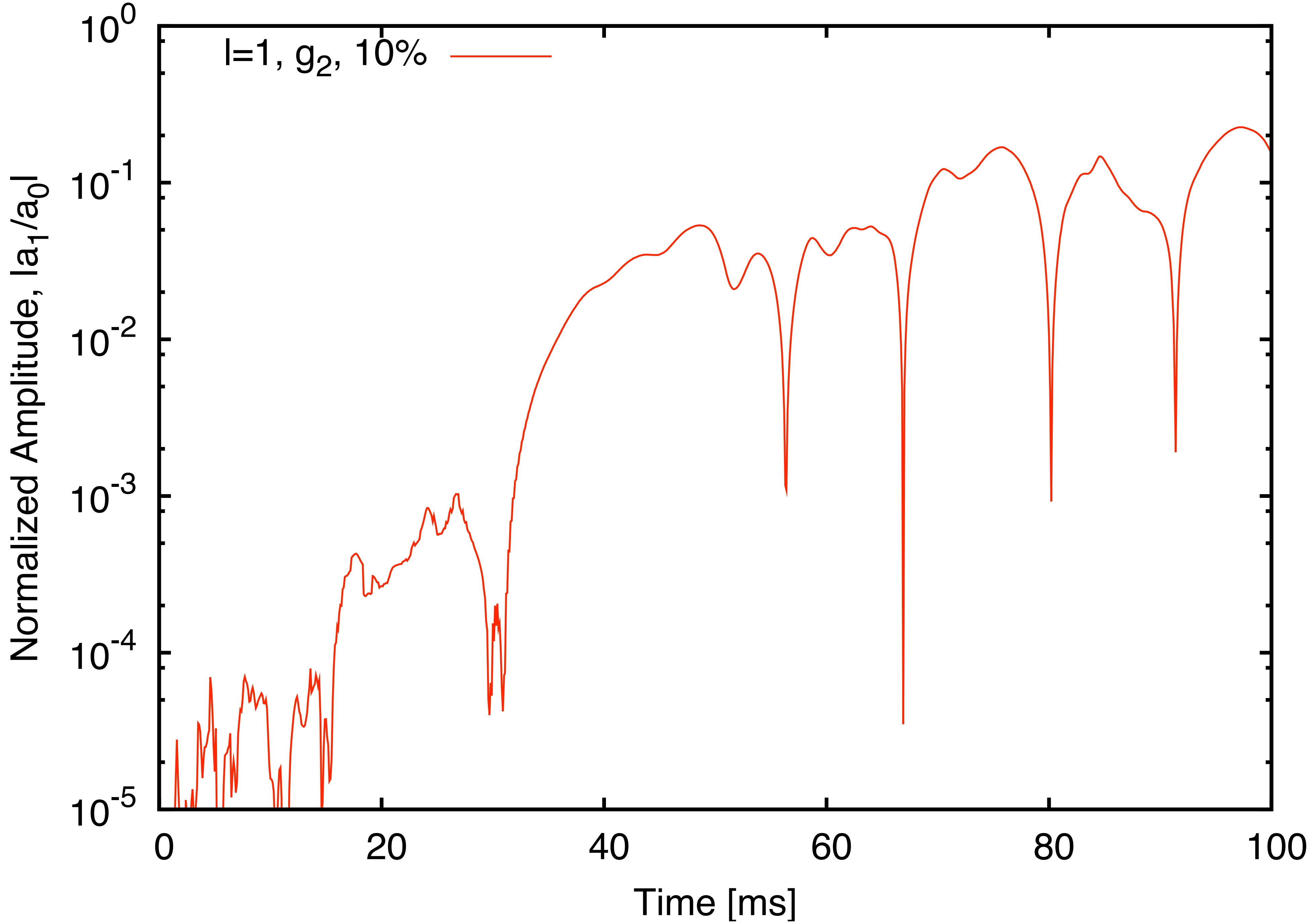

SUMMARY

Standing accretion shock instability has been investigated by 2D axisymmetric simulations with steady-state solution

- **Linear growth of the perturbation was found for low-l modes with neutrino heating**
- **2D axisymmetric simulations suggest that SASI can trigger the explosion from the stalled shock wave**
- **Additional neutrino heating of neutrino-He inelastic scattering is enhanced by SASI but may play a minor role on a successful explosion**
- **It seems to be difficult that the pressure perturbation which is mimic of g-mode excites SASI due to the impedance mismatch**